

## Chapter 2

# Literature Review

The literature review has been divided into three major sections and each section reviews and analyzes the prior research that discusses the related work. The information presented here gives a summarized overview and help us in exploring the metabolic processes and potential of hydrogenotrophic methanogens as well as deciphering the underlying mechanisms with the help of genome-scale engineering.

### 2.1 CO<sub>2</sub> Fixing Microbes

Carbon dioxide is an inorganic form of carbon which serves as the substrate for many autotrophic microorganisms [1]. The microbial CO<sub>2</sub> fixation can be very useful for the production of bioenergy, biodiesel, biohydrogen and biodegradable plastics. In 1940, CO<sub>2</sub> fixation by *Propionibacterium pentosaceum* was first reported by Wood and Werkman [2]. Later, CO<sub>2</sub> assimilation by various heterotrophic bacteria (*Aerobacter indologenes*, *Proteus vulgaris*, *Streptococcus paracitrovorus*, and *Staphylococcus candidus*) was reported by Werkman and Wood [3]. Since then series of efforts were made for studying CO<sub>2</sub> assimilation by microorganisms. CO<sub>2</sub> assimilating microorganisms are widespread among both archaeal and bacterial domain. Within archeal domain, they belong to phyla Euryarchaeota and Crenarchaeota. While among bacterial domain, they belong to the phyla Aquificae, Actinobacteria, Chloroflexi (green non-sulfur bacteria), Proteobacteria, Chlorobi, Firmicutes and Thermodesulfobacteria [1].

There are six major CO<sub>2</sub> fixing pathways: first, Calvin cycle or Calvin-Benson-Bassham (CBB) pathway or Reductive pentose pathway found in green plants and many autotrophic bacteria [4]. Second, Reductive TCA cycle or reverse citric acid

---

Some content of this chapter has been reproduced with permission from Nishu Goyal, Zhou Zhi, and I A Karimi. "Metabolic processes of *M. maripaludis* and potential applications", Microbial Cell Factories (2016), Vol. 15, 107

cycle found in *Thermoproteus* [5]. Third, Reductive acetyl-coenzyme A (acetyl-CoA) pathway or Wood-Ljungdahl pathway generally present in strict anaerobes because of the oxygen sensitivity of its key enzyme acetyl-CoA decarbonylase/synthase (CODH/ACS) [4, 6]. The microbial species having this pathway mainly belong to methanogens and acetogens. Fourth, 3-Hydroxypropionate pathway/Methyl-CoA pathway (3-HP) which was first reported in phototrophic green non-sulfur bacterium [7]. Fifth, 3-Hydroxypropionate/4-hydroxybutyrate cycle reported in the cell extract of *Metallosphaera sedula*, an aerobic autotrophic member of sulfolobales [8] and Last, Dicarboxylate/4-hydroxybutyrate cycle found to be operating in *Ignicoccus hospitalis* (Desulfurococcales) [9].

Till date, the biological fixation of  $\text{CO}_2$  by microalgae has been investigated for global reduction of  $\text{CO}_2$  levels [10]. However, harvest has been an expensive and problematic part of industrial production of microalga biomass. In this thesis, we explore the potential of a hydrogenotroph, *M. maripaludis*. This is a very useful model organism among hydrogenotrophic methanogens that offers several advantages. (1) Rapidly growing archaea, with a doubling time of 2 h [11]. (2) Mesophilic, grows best at 35–39 °C. (3) Robust set of genetic tools for molecular and biochemical studies. (4) Cells easy to lyse and makes the isolation of DNA and other components easier. (5) Non-pathogenic. (6) No need of biofuel harvesting.

## 2.2 *M. maripaludis*—A $\text{CO}_2$ Fixer

Methanococci are non-pathogenic, mesophilic, strictly anaerobic, hydrogenotrophic, and methanogenic archaeobacteria. They comprise four species: *M. maripaludis*, *M. vannielii*, *M. voltae*, and *M. aeolicus* [12]. In this study, we focus on *M. maripaludis* (Fig. 2.1), whose type strain *M. maripaludis* JJ was isolated from salt

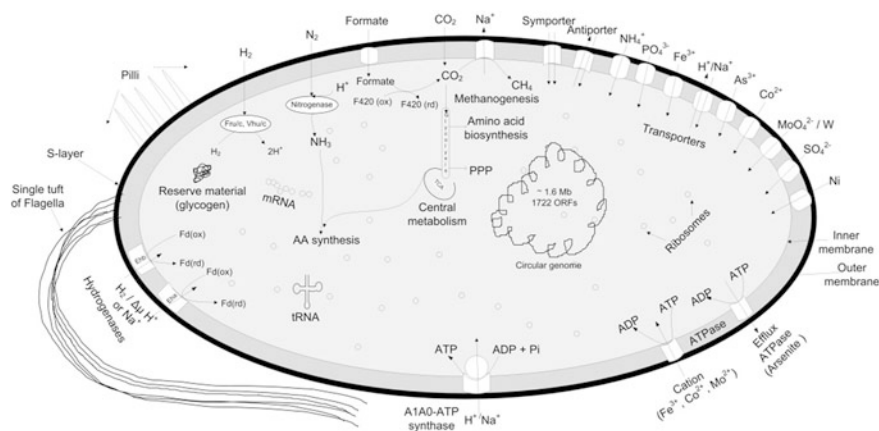


**Fig. 2.1** A schematic representation of a typical *M. maripaludis* cell

marsh sediments in South Carolina [11]. Since then, numerous strains have been isolated from estuarine sites in South Carolina, Georgia, and Florida [13]. Table 2.1 lists the characteristics of five fully sequenced strains (S2, C5, C6, C7 and X1).

*M. maripaludis* is a fast growing microbe with a doubling time of 2 h and optimum growth temperature at 38 °C. It reduces CO<sub>2</sub> to methane via a modified Wood-Ljungdahl pathway, also known as Wolfe cycle [14]. Unlike other microorganisms that need complex carbon substrates such as pentoses, hexoses, alcohols, and their derivatives for their growth, *M. maripaludis* can use simple substrates such as CO<sub>2</sub> or formate as the sole carbon sources, and N<sub>2</sub> as the sole nitrogen source [15]. However, it needs H<sub>2</sub> or formate (HCO<sub>2</sub><sup>−</sup>) as an energy source [16–18]. In other words, given a renewable source of H<sub>2</sub>,

*M. maripaludis* has the potential to convert flue gas emissions (majorly consist of CO<sub>2</sub> and N<sub>2</sub>) into a useful fuel (methane). In fact, *M. maripaludis* S2 has been a well-studied model organism in the literature [22].

In spite of more than 100 publications on the biochemistry of *M. maripaludis*, a consolidated review is missing in the literature. This chapter reviews existing literature on *M. maripaludis*, and explores its potential industrial and environmental applications. Figure 2.2 shows an overview of eight major metabolic subsystems in *M. maripaludis*: methanogenesis, reductive tricarboxylic acid (TCA) cycle, non-oxidative pentose phosphate pathway (PPP), glucose/glycogen metabolism, nitrogen metabolism, amino acid metabolism, and nucleotide metabolism.

Reduction of CO<sub>2</sub> to methane via methanogenesis is essential for the energy needs of *M. maripaludis* [23, 24], and therefore methanogenesis forms the foundation for its survival and growth. In other words, methanogenesis is coupled with cell growth, and both compete for the carbon source. The remaining seven subsystems provide the essential precursors for cell growth via two key intermediates: acetyl CoA and pyruvate.

### 2.2.1 Taxonomy, Cell Structure, and Cultivation

#### *Identification and classification*

In late 1970s, 16S rRNA gene sequences were adopted for phylogenetic analyses, and *Archaea* was classified as the third domain of life by Carl Woese and his colleagues [23]. *Archaea* is a diverse group of microorganisms widely distributed in extreme habitats, such as hot springs for the phylum Crenarchaeota and salt lakes for the phylum Euryarchaeota. The phylum Euryarchaeota includes eight classes: Methanobacteria, Methanococci, Methanomicrobia, Halobacteria, Thermoplasmata, Thermococci, Archaeoglobi, and Methanopyri. The distinctive features of the Methanococci include rapid growth in both mesophilic and thermophilic temperatures, proteinaceous S-layer as the cell envelope, and a nutritional requirement for selenium. The Methanococci include a single order Methanococcales, which includes methanogens characterized by a coccoid shape and the presence of

**Table 2.1** Characteristic features of *M. maripaludis* strains

Strains	Source/habitat	Substrate	Optimum temperature	Optimum pH	mol% GC	Growth rate (/h)	Sequenced by	Total genome size (bp)	Number of ORFs
<i>M. maripaludis</i> S2	Salt marsh sediment [13]	HCOOH, or H <sub>2</sub> and CO <sub>2</sub>	38 °C	6.8–7.2	34.4 ± 0.1	0.30	[22]	1,661,137	1772
<i>M. maripaludis</i> C5	Airport Marsh [13]	HCOOH, or H <sub>2</sub> and CO <sub>2</sub>	35–40 °C	6–8	33.1 ± 0.1	0.21	[19]	1,789,046	1889
<i>M. maripaludis</i> C6	Roger’s Marsh [13]	HCOOH, or H <sub>2</sub> and CO <sub>2</sub>	35–40 °C	6–8	34.2 ± 0.1	0.06	[19]	1,744,193	1888
<i>M. maripaludis</i> C7	Roger’s Marsh [13]	HCOOH, or H <sub>2</sub> and CO <sub>2</sub>	35–40 °C	6–8	33.7 ± 0.1	0.20	[19]	1,772,694	1855
<i>M. maripaludis</i> X1	Thermophilic saline oil reservoir [20]	HCOOH, or H <sub>2</sub> and CO <sub>2</sub>	NA	NA	32.9 ± 0.1	NA	[21]	1,746,697	1892

NA Not available

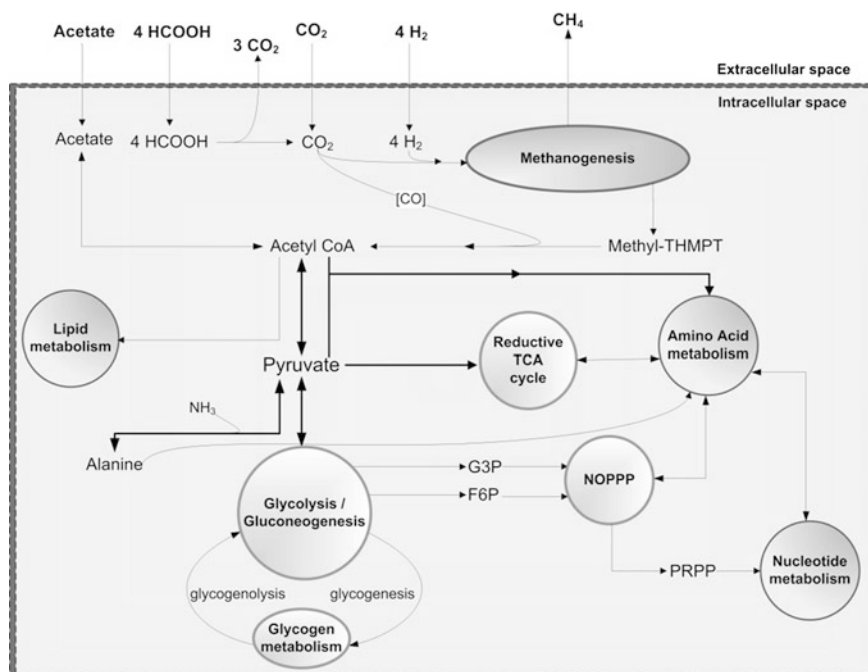


**Fig. 2.2** Simplistic overview of eight major metabolic subsystems in *M. maripaludis*

glycolipids and polar lipids in varying compositions [18]. The order Methanococcales is composed of two families: *Methanococcaceae* and *Methanocaldococcaceae*. They differ in 12 % 16S rRNA sequences and growth temperatures [25]. *Methanococcaceae* are extremely thermophilic or mesophilic, while *Methanocaldococcaceae* are all hyperthermophilic. The family *Methanococcaceae* is further subdivided into two genera, namely *Methanococcus* and *Methanothermococcus* based on their different optimum growth temperatures. The core lipid of *Methanococcus* is mainly archaeol and hydroxyarchaeol, while caldarchaeol is additionally present in *Methanothermococcus* [26]. The most abundant polyamine is spermidine in *Methanococcus* and *Methanothermococcus*. The genus *Methanococcus* is subdivided into four species, *M. aeolicus*, *M. maripaludis*, *M. vannielii*, and *M. voltae*, based on 16S rRNA sequences, DNA relatedness, cellular protein patterns, and phenotypic methods [12]. The detailed characteristics of each species have been described previously [25]. *M. maripaludis* species have five sequenced strains: *M. maripaludis* S2, *M. maripaludis* C5, *M. maripaludis* C6, *M. maripaludis* C7, and *M. maripaludis* X1, which were classified based on their 54–69 % DNA relatedness and 99.2 % sequence similarity with 16S rRNA sequences [12].

### Cell structure

*Methanococcus* has a spherical shape. Its cell wall is fragile and its morphology is affected by its physiological state and the ionic strength of growth medium. *M. maripaludis* cells are weakly-motile cocci with a diameter ranging from 0.9 to 1.3  $\mu\text{m}$  [11]. They are non-spore forming mesophile, and grow best at a temperature between 20 and 45  $^{\circ}\text{C}$  and a pH between 6.5 and 8.0 [27]. The cell envelope of *M. maripaludis* is a single electron dense layer. The cell wall is a proteinaceous S-layer, but lacks peptidoglycan molecules. The molecular mass of S-layer proteins was found to be in the range of 59,064 and 60,547 Da [28]. The proteinaceous cell wall of *M. maripaludis* lyses rapidly in low concentrations of detergents [11] and buffers of low osmolarity [29], which makes the isolation of DNA easier. Despite the differences in the predominance of some amino acids, the primary structure of S-layer proteins shows a high degree of identity (38–45 %) [28]. Ether lipids recovered from *M. maripaludis* mainly include glycolipid (14.2 mg ether lipid/g dry cell weight) and polar lipids (0.4 mg ether lipid/g dry cell weight) [30]. The S-layer proteins and flagellins of *M. maripaludis* have been discussed in the literature [31, 32].

The motility in methanococci is due to the presence of flagella. However, efficient attachments to the surfaces in *M. maripaludis* require both flagella and pili [33]. Bardy et al. [34] demonstrated the presence of *flaK* and preflagellin peptidase activity in *M. maripaludis*, but the exact role of this peptidase in the secretion of archaeal flagellins and assembly of flagella is unknown. To understand the proper assembly and function of flagella in *M. maripaludis*, Chaban et al. [35] performed systematic deletions of *fla* genes in the flagella operon that consists of three flagellin genes (*flaB1*, *flaB2*, and *flaB3*) and eight others (*flaC* to *flaJ*). Their results showed that individual deletions of *flaB1*, *flaB2*, *flaC*, *flaF*, *flaG*, *flaH* and *flaI* resulted in non-motile and non-flagellated cells. *flaJ* was homologous to the integral membrane proteins in the type IV pili system, and is necessary for flagellation in a closely related methanogen *M. voltae*. Thus, its deletion was exempted. The experiments on deletions of *flaD* and *flaE* failed several times for unknown reasons, which requires further research [36]. Interestingly, an acetyltransferase gene involved in sugar biosynthesis in *M. maripaludis* was found to affect flagellin N-linked glycosylation and proper assembly of both flagella and pili [37]. The deletion of this gene resulted in completely nonglycosylated flagellins and defective pilus anchoring [37]. The composition of a novel N-linked flagellar glycan in *M. maripaludis* was identified in 2009 [38]. A genetic analysis for the type IV pili formation in *M. maripaludis* was conducted, but specific roles of these pili are still unknown [39]. However, if archaeal pili are similar to bacterial pili, then archaeal pili could be involved in functions related to cell-to-cell twitching motility, attachment, biofilm formation, etc.

### Growth media, Culture conditions, and Storage

*M. maripaludis* is a routinely cultured hydrogenotrophic methanogen. It can grow anaerobically on minimal medium (McN), complex medium (McC), and minimal

medium plus sodium acetate (McNA) [13]. Plate colonization of *M. maripaludis* on solidified agar medium with 50–100 % plating efficiency and maximum colony size was achieved by optimizing the inoculation method, H<sub>2</sub>S concentration, and agar moisture content [40]. The preferred carbon and energy source is CO<sub>2</sub>–H<sub>2</sub> (20:80 v/v) at a pressure of about 275 kPa. In the absence of H<sub>2</sub>, formate can serve as the sole carbon and energy source in the presence of N<sub>2</sub>–CO<sub>2</sub> (80:20 v/v) [41, 42]. However, excess of either H<sub>2</sub> or formate decreases the ratio of growth yield to methane significantly [17].

Amino acids and vitamins may affect [43] the growth rate and cell yield (mg dry cell weight/ml) of methanococci. Some of the facultative autotrophic strains, such as Strain D1, Strain C5, Strain C9, and Strain C14, assimilated large amounts of amino acids, but the growths of *M. vannielli* and *M. aeolicus* were unaffected. The growth of *M. maripaludis* was moderately stimulated, possibly because *M. maripaludis* was capable of utilizing alanine as the sole nitrogen source in the absence of other nitrogen sources, while *M. vannielli* and *M. aeolicus* could not use alanine as the sole nitrogen source. Although exogenous amino acids can substitute for 40–60 % of the total cell carbon by some autotrophic methanococci, they were not the major nitrogen sources and were not extensively metabolized. The growth of 16 autotrophic isolates, such as *M. maripaludis*, *M. vanniellii*, *M. deltae*, and *M. aeolicus*, remained unaffected by the mixture of water soluble vitamins [43]. Pantothenate was the only vitamin that stimulated the growth of *M. voltae* [44].

Long-term storage of *M. maripaludis* cultures in glycerol stock solutions has been reported [13]. Cultures were grown to the early stationary phase, concentrated by centrifugation, and cell pellets were resuspended in media containing 25 % glycerol and then stored at –70 °C. The addition of glycerol stabilizes frozen microorganisms, prevents damage to cell membranes, and keeps the cell alive for many years.

## 2.2.2 *Metabolic Processes in M. maripaludis*

In this section, we focus on metabolic processes, energy production, and genome-scale modeling. Specifically, we discuss methanogenesis, acetyl-CoA synthesis, pyruvate synthesis, glycolysis/gluconeogenesis, reductive tricarboxylic acid (TCA) cycle, non-oxidative pentose phosphate pathway (PPP), nitrogen metabolism, amino acid metabolism, nucleotide metabolism, molecular biology tools, genome-scale model, and applications.

### 2.2.2.1 Methanogenesis

Methanogenesis (Fig. 2.3) is the biological production of methane from the reduction or disproportionation of simple carbon substrates (e.g. CO<sub>2</sub>, formate, acetate and methanol) as per the following reactions:

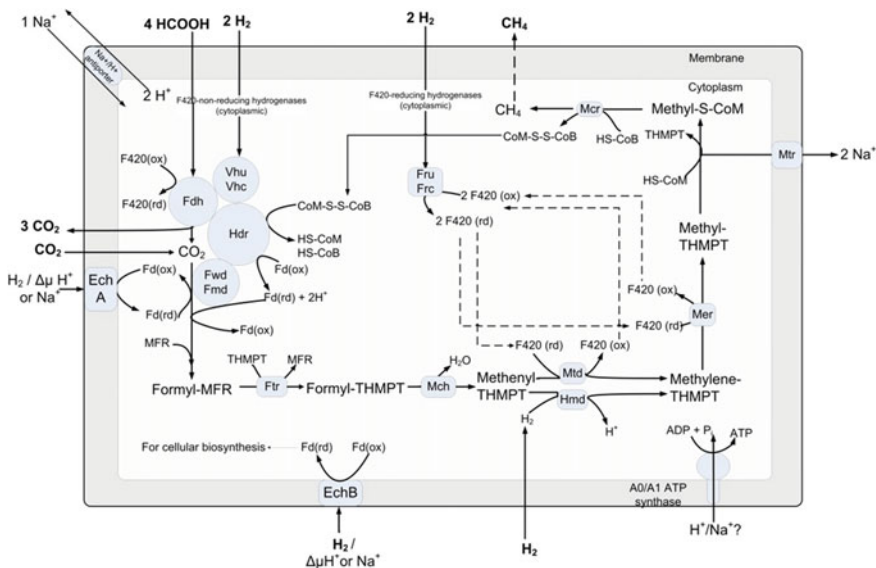
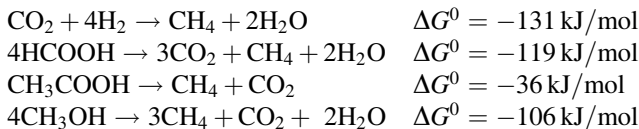


**Fig. 2.3** Energy producing pathway in *M. maripaludis*



While formate, acetate, and methanol oxidize/reduce by themselves,  $\text{CO}_2$  needs an electron donor such as  $\text{H}_2$  [11], formate [41], or electricity [45]. In *M. maripaludis*, methanogenesis can occur via the reduction of  $\text{CO}_2$  with  $\text{H}_2$ /formate/electricity, or the disproportionation of formate. Lohner et al. [45] demonstrated  $\text{H}_2$ -independent electromethanogenesis from  $\text{CO}_2$  in both wild-type *M. maripaludis* strain S2 and hydrogenase mutant strain MM1284. Mutant strain under the same conditions reduced methane production rates by a factor of 10 compared to those observed with the wild-type strain S2 [45]. However, the attempts to quantify biomass growth were inconclusive.

The formate-dependent methanogenesis involves an additional endergonic step where formate is oxidized to  $\text{CO}_2$  via formate dehydrogenase with a simultaneous reduction of coenzyme F420 [42]. The reduced coenzyme F420 serves as the electron carrier for two intermediary steps in methanogenesis. However,  $\text{H}_2$  is probably not an intermediate during formate-dependent methanogenesis [41, 46]. As shown in Fig. 2.3, the resulting  $\text{CO}_2$  participates in the first step of methanogenesis.

A recent study [17] showed the effects of  $\text{H}_2$  and formate limitation/excess on growth yield and regulation of methanogenesis using a continuous culture of *M. maripaludis*. They concluded that the growth yield (g dry cell weight



(DCW)/mol CH<sub>4</sub>) decreased remarkably with excess H<sub>2</sub> or formate. While they speculated energy spilling or dissipation to be a possible cause, the exact cause is still unclear. While *M. maripaludis* can also assimilate other carbon substrates, such as acetate and pyruvate, they are not the physiologically relevant substrates for methane production [47, 48]. No methane production from acetate (17), and extremely low methane (only 1–4 % compared to that for H<sub>2</sub>) has been reported from pyruvate [48].

### **Mechanism**

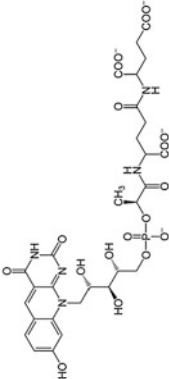
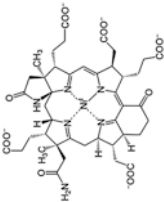
The structures and functions of the cofactors and coenzymes involved in methanogenesis are listed in Table 2.2. The first step in methanogenesis is the reduction of CO<sub>2</sub>. It involves the simultaneous oxidation of low-potential reduced ferredoxins and the capture of CO<sub>2</sub> by methanofuran (MFR) to form formyl-MFR ( $\Delta G^0 = 0$  kJ/mol) [55]. These extremely low-potential ferredoxins could come from two pools [56]. One is EchA that not only uses one H<sub>2</sub>, but also consumes proton-motive force (PMF) to generate ferredoxins. This accounts for only 4 % of the reduce ferredoxins as shown in a  $\Delta 5H_2ase$  mutant [46]. The second and the major pool is Vhu/Hdr bifurcation complex that consumes two H<sub>2</sub> and generates one pair of relatively high potential electrons to reduce CoB-S-S-CoM and another pair of extremely low potential electrons to reduce the ferredoxins. The formyl group from formyl-MFR is then transferred to THMPT ( $\Delta G^0 = -5$  kJ/mol) to form formyl-THMPT, and the latter is then dehydrated to methenyl-THMPT ( $\Delta G^0 = -5$  kJ/mol) [57]. In the next two steps, the reduced F420 supplies electrons to reduce methenyl-THMPT to methylene-THMPT ( $\Delta G^0 = +6$  kJ/mol) and methylene-THMPT to methyl-THMPT ( $\Delta G^0 = -6$  kJ/mol) [58]. These reactions are fully reversible, as evidenced by their near zero free energy changes. The oxidized F420 is then reduced ( $\Delta G^0 = -11$  kJ/mol) in the presence of H<sub>2</sub> [55]. Next, the methyl group from methyl-THMPT is transferred to coenzyme M (HS-CoM) in an exergonic step ( $\Delta G^0 = -30$  kJ/mol) coupled with 2Na<sup>+</sup> translocation by a membrane-bound enzyme complex [59]. This reaction builds up an electrochemical Na<sup>+</sup> gradient, which drives energy production via ATP synthase [55]. The final step of methanogenesis is the reductive demethylation of methyl-S-CoM to methane and CoM-S-S-CoB ( $\Delta G^0 = -30$  kJ/mol). Subsequently, this CoM-S-S-CoB gets reduced with the help of H<sub>2</sub> to form HS-CoM and HS-CoB ( $\Delta G^0 = -39$  kJ/mol) [60]. This reduction of CoM-S-S-CoB mediates via an electron bifurcation mechanism [55]. This step along with the earlier step involving the Na<sup>+</sup> translocation supplies the major energy demand of *M. maripaludis*.

### **Hydrogenases**

The key to the survival of *M. maripaludis* on CO<sub>2</sub> is its ability to take up external H<sub>2</sub> and perform  $H_2 \rightarrow 2H^+ + 2e^-$  with the help of seven hydrogenases (Fig. 2.3). These are Fru, Frc, Vhu, Vhc, Hmd, EchA, and EchB, which can be categorized in different manners. The first five are cytoplasmic and the last two are membrane-bound [61]. Fru and Frc use cofactor F420 [53], Vhu and Vhc use



Table 2.2 (continued)

Cofactor/coenzyme	Structure	Function	Reference
Coenzyme F420		Major electron transfer currency. Transfer electrons from H <sub>2</sub> to the consecutive intermediates of methane biosynthesis e.g. coenzyme F420 hydrogenase, 5,10-methylene-THMPT reductase and methylene-THMPT dehydrogenase	[50, 53]
Cofactor F430		This cofactor is the prosthetic group of the methyl-CoM reductase which catalyzes the release of methane and CoB-S-S-CoM in the final step of methanogenesis	[50, 54]

ferredoxin and CoM/CoB [62], Hmd uses direct  $H_2$  [53], and EchA and EchB use ferredoxins as electron carriers [46]. *M. maripaludis* needs four pairs of electrons to reduce one mole of  $CO_2$  to methane. Fru/Frc can supply two pairs, Vhu/Vhc can supply two pairs, Hmd can supply one pair, and EchA/EchB can supply one pair each. Of these, Fru/Frc and Vhu/Vhc play a major role in  $H_2$  uptake.

Fru and Frc reduce two molecules of coenzyme F420 with the help of two  $H_2$  [53]. One F420(rd) gets oxidized by reducing methenyl-THMPT and the other by reducing methylene-THMPT.

Vhu and Vhc facilitate the flow of electrons from  $H_2$  to heterodisulfide reductase (Hdr) complex [62], which in turn catalyzes the reductions of CoM/CoB and ferredoxins via an electron bifurcation mechanism [60]. These reduced ferredoxins are the major electron suppliers during the first step of methanogenesis.

Hmd uses  $H_2$  to reduce methenyl-THMPT to methylene-THMPT [53] without any carrier. As shown in Fig. 2.3, Mtd also catalyzes the same reaction, but with the help of reduced F420 as an electron carrier. Hendrickson et al. [53] demonstrated that during the growth on  $H_2$  and  $CO_2$ , Hmd is not essential in the presence of active Fru/Frc, but it is essential otherwise. In contrast, the  $\Delta$ Fru,  $\Delta$ Frc, and  $\Delta$ Hmd mutants grew normally during formate-dependent growth.

EchA generates a small portion of low-potential reduced ferredoxins required for the first step of methanogenesis. Its role in *M. maripaludis* is anaplerotic, because it is required only under certain conditions such as (1) to replenish the intermediates of methanogenesis cycle, and (2) imperfect coupling during electron bifurcation [46]. Lie et al. [46] showed this by eliminating all nonessential pathways of  $H_2$  metabolism and using formate as the sole electron donor. In this case, both Hdr complex and EchA independently provided electrons for growth.

In contrast, EchB supplies electrons to anabolic oxidoreductases for the synthesis of precursors such as pyruvate and acetyl CoA [61, 215]. EchB mutants affect the autotrophic growth severely, but it is unclear how they still survive. When conditions limit growth, anabolic  $CO_2$  fixation is unimportant, but methanogenesis continues. Under such a scenario, EchA is essential, but EchB could be detrimental [46].

During formate-dependent growth, the  $H_2$  required for the essential anaplerotic (EchA) and anabolic (EchB) functions has to be produced from formate. This  $H_2$  production can occur via two pathways as demonstrated by Lupa et al. [42] in *M. maripaludis*. One involves Fdh1-Fru/Frc, and the other involves Fdh1-Mtd-Hmd. Of these, the former seems to be predominant ( $\sim 90\%$ ), as the deletion of either Fdh1 or Fru/Frc reduced  $H_2$  production rates severely.

### **Energy Generation/Conservation**

In most organisms, electron movement along the cell membrane is the key to energy transduction. Substrate oxidation releases electrons that move along the membrane-bound cytochrome carriers and extrudes protons out of the cell to generate a potential gradient. The potential difference drives the protons back into the cell, while synthesizing ATP from ADP and  $P_i$  via ATP synthase [63].

Hydrogenotrophic methanogens such as *M. maripaludis* lack such an electron transport chain [64]. In place of cytochrome carriers, *M. maripaludis* uses methyl-THMPT: HS-COM methyltransferase (Mtr), the only membrane-bound enzyme complex in the core methanogenic pathway, to extrude Na<sup>+</sup>/H<sup>+</sup> out of the cell [55, 59]. This creates a Na<sup>+</sup>/H<sup>+</sup> ion motive force (positive outside), which on their translocations into the cell generate ATP via an A1A0-type ATP synthase [65]. However, a direct experimental evidence specifically for Na<sup>+</sup> or H<sup>+</sup> gradient does not exist in the literature for *M. maripaludis*. To conserve ATP, *M. maripaludis* uses reduced ferredoxins as low-potential electron carriers for the highly endergonic reduction of CO<sub>2</sub> to formyl-MFR. As discussed earlier, these ferredoxins are supplied predominantly by the Hdr complex [60] and supplemented by EchA.

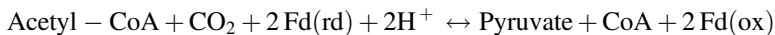
The genome sequence of *M. maripaludis* indicates the presence of membrane-bound A1A0-type ATPases (chimeric ATP synthases) instead of the F1F0-type ATPases found in Bacteria and Eukarya [22, 66]. The catalytic unit of the A1A0-type ATPase is structurally homologous to the V-type ATPase and functionally homologous to the F1F0-type ATPase [67]. But, the membrane-embedded motors in the A1A0-type ATP synthases are exceptional due to their novel functions and structural features [68].

### 2.2.2.2 Acetyl-CoA Synthesis

*M. maripaludis* can synthesize acetyl-CoA from either CO<sub>2</sub> or acetate [16, 47]. The CO<sub>2</sub>-based synthesis occurs with the help of CODH/ACS [16]. Sequencing studies have confirmed the existence of CODH/ACS in a single cluster (MMP0980-MMP0985) [22]. During the CO<sub>2</sub>-based synthesis, methyl-THMPT, an intermediate of methanogenesis, contributes the methyl carbon of acetyl-CoA while CO, which is generated during reduction of CO<sub>2</sub> in the presence of reduced ferredoxins by CO dehydrogenase (CODH), contribute the carboxyl carbon [16]. The acetate-based synthesis is accomplished by AMP-forming acetate CoA ligase (MMP0148, *acsA*) in *M. maripaludis* [47]. Shieh et al. [47] showed that *M. maripaludis* can assimilate up to 60 % of its cellular carbon from exogenous acetate. Sequencing study also showed the presence of ADP-forming acetyl-CoA synthetase gene (MMP0253, *acd*) in *M. maripaludis* [22], catalyzes acetate formation and ATP synthesis from acetyl CoA, ADP and Pi. However, no experimental study exists in the literature to demonstrate the biosynthesis of free acetate by *M. maripaludis*.

### 2.2.2.3 Pyruvate Synthesis

Pyruvate is the entry point into glycolysis, citric acid cycle, and amino acid metabolism. Acetyl-CoA is converted to pyruvate through pyruvate: ferredoxin oxidoreductases (PORs) [53, 69, 70] as follows:



This is reversible in that PORs also catalyze pyruvate oxidation to acetyl-CoA in the absence of  $\text{H}_2$  [48]. However, pyruvate oxidizes very slowly in *M. maripaludis* and PORs appear to function mainly in the anabolic directions during growth [69].

The PORs containing five polypeptides in *M. maripaludis* are encoded by a gene cluster (*porABCDE*). Of these, *porEF* is unique to *M. maripaludis*, because the N-terminal sequences of the first four polypeptides (*porABCD*) are similar to those in other *Archaea* [70]. The importance of *porEF* in *M. maripaludis* was highlighted by Lin et al. [71]. They showed that *porEF* mutants of *M. maripaludis* JJ grew extremely slowly. In addition, pyruvate-dependent methanogenesis was completely inhibited. Interestingly, *porF* mutant failed to restore growth, but restored methanogenesis to wild-type levels. In contrast, *porE* mutant restored growth partially, but did not restore methanogenesis. This indicates that *porF* function as an electron donor to PORs.

Pyruvate is also a precursor for alanine biosynthesis via alanine dehydrogenase (MMP1513, *ald*) [72]. The same enzyme catalyzes the reverse reaction also, i.e. alanine to ammonia and pyruvate, in *M. maripaludis*. In addition, alanine transaminase that catalyzes the conversion of alanine to pyruvate in several organisms including *Pyrococcus furiosus*, *Escherichia coli*, *Mus musculus*, and *Homo sapiens*, may also exist in *M. maripaludis*. Our inference is based on our BLASTp search with the protein sequences of *M. maripaludis*. Our search located proteins with high similarity (E-value =  $7\text{e-}63$ ) to the alanine transaminase from *P. furiosus*. *M. maripaludis* takes alanine with the help of alanine permease and alanine racemase. While the former transports both L-alanine and D-alanine into the cell, the latter is essential to convert D-alanine to L-alanine [72, 73], because alanine dehydrogenase is specific for L-alanine.

#### 2.2.2.4 Glycolysis/Gluconeogenesis and Glycogenolysis/Glyconeogenesis

*M. maripaludis* does not assimilate carbohydrates such as pentoses and hexoses, as it lacks the required transporters [22]. However, it has all the enzymes and cofactors required for glycolysis/gluconeogenesis and glycogenolysis/glyconeogenesis with some unique features. In fact, studies have shown that methanococci such as *M. maripaludis* synthesize and store glycogen as a reserve metabolite, and use it for methane generation in the absence of exogenous substrates [74]. The bifunctional activity of ADP-dependent phosphofructokinase (PFK)/glucokinase (GK) has been demonstrated experimentally in both *M. jannaschii* [75] and *M. maripaludis* [76]. Castro-Fernandez et al. [76] measured the activities of glucose phosphorylation versus dephosphorylation. They unexpectedly observed that the latter was 2-folds more efficient than the former. Based on these observations, they indicated that

*M. maripaludis* can catalyze D-glucose formation, and suggested the possibility of methane production from glycogen or D-glucose during starvation in *M. maripaludis*.

Unlike non-methanogenic *Archaea* that use ED pathway, *M. maripaludis* [74] uses a modified Embden-Meyerhof-Parnas (EMP) pathway with some unique features. These include the reduction of ferredoxins instead of NAD (e.g. PORs and GAPOR) [77], ADP-dependent kinases [75], zero or very low ATP yields [78], highly divergent phosphoglucose isomerase [79], and phosphoglycerate mutase [80]. Of the eight enzymatic steps (5–13) from pyruvate to glucose-6-phosphate (Fig. 2.4), five are reversible and catalyzed by the same enzyme, and the rest are irreversible (5, 9, and 12). However, even for these three irreversible steps, reverse steps are catalyzed by alternative enzymes [phosphoenolpyruvate synthase (PPS), glyceraldehyde-3-phosphate dehydrogenase (GAPDH), and fructose-bisphosphatase (FBP)]. In other words, all the steps leading to glucose-6-phosphate from pyruvate are reversible in principle. Glycogen in *M. maripaludis* is then synthesized by converting (1) glucose-6-phosphate to glucose-1-phosphate via phosphoglucomutase

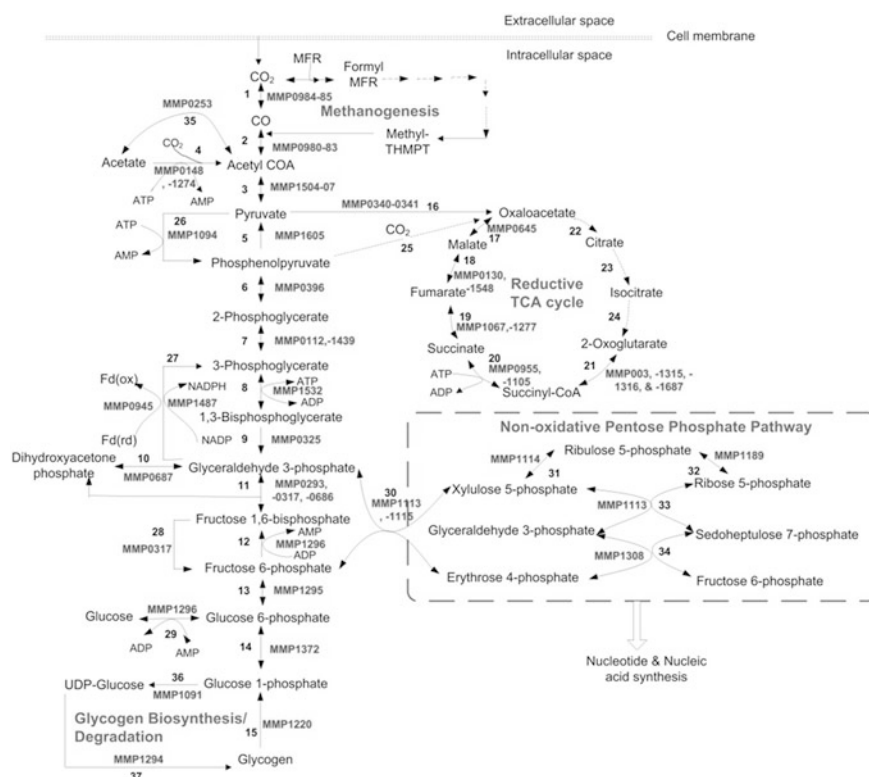


**Fig. 2.4** Diagram outlining the reactions and associated ORF and enzymes involved in glycolysis/gluconeogenesis, TCA, and PPP of *M. maripaludis*

(MMP1372), (2) glucose-1-phosphate to UDP-glucose via UTP-glucose-1-phosphate uridylyltransferase (MMP1091), and (3) the growing polymeric chain of UDP-glucose to glycogen via glycogen synthase (MMP1294) with the release of UDP molecule [22]. On the other hand, glycogen in *M. maripaludis* degrades to glucose-6-phosphate by converting (1) glycogen to glucose-1-phosphate via glycogen phosphorylase (MMP1220), and (2) glucose-1-phosphate to glucose-6-phosphate via glucose phosphomutase (MMP1372) [22, 74]. The low activity of PFK in comparison to FBP in *M. maripaludis* suggests that glycconeogenesis is the predominant function of EMP pathway in *M. maripaludis* pointing to the storage of glycogen as a reserve material [74]. This predominance of the anabolic direction is further confirmed by the high activities of the reversible hexose phosphate conversions (via glucose phosphomutase, glucose-6-phosphate isomerase, and fructose-bisphosphate aldolase) and triose phosphate conversions for pentose biosynthesis (via enolase, 2,3-bisphosphoglycerate mutase, and glyceraldehyde-3-phosphate dehydrogenase). Yu et al. [74] further showed that glycogen content increased from 0.11 %  $\pm$  Solid lines show the presence of enzymes and dotted lines show the absence of enzyme in *M. maripaludis*. Numbers mentioned in diagram indicate enzymes as follows: 1. carbon-monoxide dehydrogenase (1.2.7.4, *codh* and *porEF*); 2. acetyl CoA decarbonylase (2.1.1.245, *acds*); 3. pyruvate:ferredoxin oxidoreductase/synthase (1.2.7.1, *porABCD*); 4. acetyl CoA synthetase (AMP forming) (6.2.1.1, *acsA*); 5. phosphoenolpyruvate kinase (2.7.1.40, *pyk*); 6. enolase (4.2.1.11, *eno*); 7. 2,3-bisphosphoglycerate mutase (5.4.2.12, *pgm*); 8. phosphoglycerate kinase (2.7.2.3, *pgk*); 9. glyceraldehyde-3-phosphate dehydrogenase (1.2.1.59, *gapdh*); 10. triosephosphate isomerase (5.3.1.1, *tpi*); 11. fructose-bisphosphate aldolase (4.1.2.13, *fbp*); 12. phosphofructokinase (2.7.1.147, *pfk*); 13. glucose-6-phosphate isomerase (5.3.1.9, *pgi*); 14. Phosphoglucomutase (5.4.2.8, *pgm*); 15. glycogen phosphorylase (2.4.1.1, *glgP*); 16. pyruvate carboxylase (6.4.1.1, *pycB*); 17. malate dehydrogenase (1.1.1.37, *mdh*); 18. fumarate hydratase (4.2.1.2, *fumA*); 19. succinate dehydrogenase/fumarate reductase (1.3.5.4/1.3.4.1, *sdhA*); 20. succinyl-CoA synthetase (6.2.1.5, *sucC* and *sucD*); 21. 2-oxoglutarate oxidoreductase (1.2.7.3, *korABDG*); 22. citrate synthase; 23. aconitate; 24. isocitrate dehydrogenase; 25. phosphoenolpyruvate carboxylase; 26. phosphoenolpyruvate synthase (2.7.9.2, *ppsA*); 27. NADP-dependent glyceraldehyde-3-phosphate dehydrogenase (1.2.1.9, *gapn*) OR ferredoxin-dependent glyceraldehyde-3-phosphate dehydrogenase (1.2.7.6, *gapor*); 28. fructose-bisphosphatase (3.1.3.11, *fbp*); 29. ADP-specific phosphofructokinase (2.7.1.147, *pfk*); 30. transketolase (2.2.1.1, *tkl*); 31. ribulose-phosphate 3-epimerase (5.1.3.1, *rpe*); 32. ribose-5-phosphate isomerase (5.3.1.6); 33. transketolase (2.2.1.1, *tkl*); 34. transaldolase (2.2.1.2, *tal*); 35. Acetate CoA synthetase (ADP-forming) (6.2.1.13, *acd*); 36. UTP-glucose-1-phosphate uridylyltransferase (2.7.7.9); 37. starch synthase (2.4.1.21, *glgA*)

0.05 % DCW ( $A_{660} \leq 0.5$ ) to 0.34 %  $\pm$  0.19 % DCW ( $A_{660}$  1.0–1.6) during growth, while glycogen consumption depended on the substrate for methanogenesis.

Given the key role of glycolysis/glyconeogenesis in *M. maripaludis*, it is critical to understand their regulation. In general, a pathway can be regulated by (1) substrate availability, (2) up- or down-regulating enzyme activities for rate-limiting



steps, (3) allosteric regulation of enzymes, and (4) covalent modifications of substrates such as phosphorylations. Essentially, the enzymes catalyzing irreversible steps are most suited for regulation [81]. In most *Archaea*, nonphosphorylating NADP<sup>+</sup>-dependent glyceraldehyde-3-phosphate (G3P) dehydrogenase (GAPN), phosphorylating glyceraldehyde-3-phosphate dehydrogenase (GAPDH), and glyceraldehyde-3-phosphate ferredoxin oxidoreductase (GAPOR) act as the regulatory points in glycolysis [82–84]. The genome sequence of *M. maripaludis* codes for all three genes, namely GAPN (MMP1487), GAPDH (MMP0325), and GAPOR (MMP0945) [22]. GAPOR catalyzes ferredoxin-dependent G3P oxidation, GAPN catalyzes NADP-dependent G3P oxidation, and GAPDH catalyzes G3P synthesis. Based on activity, transcript, and flux balance analyses in *M. maripaludis*, Park et al. [85] showed that GAPOR is a post-transcriptionally regulated enzyme that is completely inhibited by the presence of 1  $\mu$ M ATP, and (unlike GAPN) is most likely involved only under non-optimal growth conditions.

Yu et al. [74] mentioned pH-dependent PFK (optimum pH = 6.0) as an important regulatory enzyme in *M. maripaludis*. The activation and inhibition of PFK was found to be dependent on the presence/absence of various substrates such as ADP, AMP, Pi, cAMP, and citrate. Yu et al. [74] also reported that full activity of pyruvate kinase, another key enzyme in glycolysis, depended on Mn<sup>2+</sup>. In contrast to Mn<sup>2+</sup>, Fe<sup>2+</sup> showed 70 % activity, and Mg<sup>2+</sup> showed 20 % activity of pyruvate kinase, while Zn<sup>2+</sup>, Cu<sup>2+</sup>, Co<sup>2+</sup>, and Ni<sup>2+</sup> showed zero activity. The activity of phosphoglycerate mutase was unaffected by Mg<sup>2+</sup> and AMP, and depended on the presence of reduced dithiothreitol, cysteine hydrochloride, and glutathione.

### 2.2.2.5 Tri-Carboxylic Acid (TCA) Cycle

TCA cycle plays an important role in generating electron carriers such as NADH and FAD for energy production [86]. Most aerobes have an oxidative TCA cycle to oxidize complex carbon molecules, such as sugars, to CO<sub>2</sub> and H<sub>2</sub>O to generate energy [86]. However, most anaerobes have reductive TCA cycles to reduce CO<sub>2</sub> and H<sub>2</sub>O to synthesize carbon compounds. Methanogens being anaerobes also have reductive TCA cycles. Furthermore, their TCA cycles are incomplete, as they lack several steps and enzymes [87]. *M. maripaludis* in particular lacks phosphoenolpyruvate carboxykinase, citrate synthase, aconitate, and isocitrate dehydrogenase [47, 88]. The missing steps in *M. maripaludis* are shown as dashed lines in Fig. 2.4. As shown, pyruvate is the entry metabolite in *M. maripaludis* for TCA cycle. In the absence of phosphoenolpyruvate carboxylase (PPC), *M. maripaludis* converts pyruvate to oxaloacetate via pyruvate carboxylase (PYC). Oxaloacetate is then reduced to 2-oxoglutarate via a series of intermediates (Malate, Fumarate, Succinate, Succinyl CoA) in the TCA cycle. Hendrickson et al. [22] sequenced the genome of *M. maripaludis* and noted that 2-oxoglutarate oxidoreductase, the last enzyme in the TCA cycle has four subunits (MMP0003, MMP1315, MMP1316, and MMP1687) that are not contiguous. This is in contrast to PORs that are also oxidoreductases, but have contiguous subunits (MMP1502-MMP1507).

Regulation of TCA cycle in *M. maripaludis* in particular, and *Archaea* in general, is poorly understood. However, 2-oxoglutarate plays an important role in nitrogen regulation [89]. In *M. maripaludis*, NrpR protein represses N<sub>2</sub>-fixation in ammonia-rich conditions by binding to the *nif* promoters [90]. In the absence of ammonia, 2-oxoglutarate is unable to synthesize glutamate, hence its level increases. High levels of 2-oxoglutarate acts as the inducer and prevents binding of NrpR to *nif* promoters, resulting in activation of N<sub>2</sub>-fixation and glutamine synthetase to bring down 2-oxoglutarate levels.

The TCA regulation in *Methanobacterium thermoautotrophicum*, another methanogen with an incomplete reductive cycle similar to that in *M. maripaludis*, can shed some light on the regulation. As reported by Eyzaguirre et al. [58] for *M. thermoautotrophicum*, *M. maripaludis* may also exhibit unidirectional synthesis of phosphoenolpyruvate via phosphoenolpyruvate synthetase (*ppsA*). The activity of this enzyme may be inhibited by AMP, ADP, and 2-oxoglutarate. Similarly, PYC, the ATP-dependent enzyme responsible for pyruvate carboxylation in *M. maripaludis*, may exhibit anabolic function as reported by Mukhopadhyay et al. [58] in *M. thermoautotrophicum*. Furthermore, its activity may depend on biotin, ATP, Mg<sup>2+</sup> (or Mn<sup>2+</sup>, Co<sup>2+</sup>), pyruvate, and bicarbonates, and it may be inhibited by ADP and 2-oxoglutarate.

#### 2.2.2.6 Pentose Phosphate Pathway (PPP)

PPP is essential for the syntheses of nucleotides and nucleic acids in *M. maripaludis*. Glyceraldehyde-3-phosphate and fructose-6-phosphate synthesized during glycolysis/gluconeogenesis form the feeds to PPP and produce xylulose-5-phosphate and erythrose-4-phosphate (E4P) via transketolase (TKL) in the first step. Yu et al. [68] proposed a non-oxidative PPP (NOPPP) in *M. maripaludis* (Fig. 2.4). They suggested the presence of this pathway based on zero activities of oxidative enzymes [glucose-6-phosphate dehydrogenase and 6-phosphogluconate dehydrogenase] and high activities of non-oxidative enzymes [transketolase (MMP1113, MMP1115), transaldolase (MMP1308), ribose-5-phosphate 3-epimerase (MMP1114), and ribulose-5-phosphate isomerase (MMP1189)] [22, 74]. Tumbula et al. [91] supported this observation by ruling out oxidative PPP based on the labelling patterns of riboses after supplementing the medium with 2-<sup>13</sup>C acetate. They argued that E4P cannot be the precursor for aromatic amino acids (AroAAs), if NOPPP is its only route. Therefore, they conjectured an alternative route (carboxylation of a triose such as dihydroxyacetone phosphate) for E4P. Porat et al. [92] on the other hand showed that E4P is not a precursor for AroAAs in *M. maripaludis*. They proposed two alternative routes for the syntheses of AroAAs based on the presence of dehydroquinase dehydratase. The details of these routes are provided in the amino acid metabolism. NOPPP is mainly regulated by substrate availability [93, 94]. However, no such regulation has yet been demonstrated in *M. maripaludis*.

### 2.2.2.7 Nitrogen Metabolism

*M. maripaludis* is capable of utilizing three nitrogen sources: ammonia, alanine, and free nitrogen with ammonia being the most preferred source for growth [72, 95].

Ammonia assimilation occurs in *M. maripaludis* via glutamine synthetase (encoded by *glnA*) which synthesizes glutamine from glutamate and ammonia [96]. Glutamine then serves as the precursor for protein synthesis. Cohen-Kupiec et al. [96] observed that *glnA* mutants are unable to grow even in the presence of exogenous glutamine and alanine indicating the essentiality of *glnA* and absence of glutamine transporters. As discussed before, alanine uptake occurs in *M. maripaludis* via alanine racemase and alanine permease [72]. Moore et al. [72] confirmed that alanine converts to pyruvate and ammonia by alanine dehydrogenase.

Free N<sub>2</sub> fixation in methanogens including *M. maripaludis* has been well established and extensively reviewed in the literature [97, 98]. A comparison of four N<sub>2</sub>-fixing hydrogenotrophic methanococci (*M. formicicus*, *M. maripaludis*, *M. aeolicus*, and *M. thermolithotrophicus*) is given in Table 2.3 [95, 99–101]. Blank et al. [102] studied N<sub>2</sub> fixation in wild-type *M. maripaludis* and its four mutants using transposon insertion mutagenesis. Kessler et al. [103] characterized the *nif* gene cluster in *M. maripaludis* based on sequence analysis. Six *nif* genes (*nifH*, D, K, E, N, and X) and two homologues of bacterial nitrogen sensor-regulator *glnB* (*i* and *ii*) lie between *nifH* and *nifD* in a single operon in *M. maripaludis* (Fig. 2.5a). Although the conserved order of *nif* genes resembles that in *Bacteria*, the presence of single operons and two homologues between *nif* genes is unique to *Archaea*.

As shown in Fig. 2.5b, N<sub>2</sub> fixation is effected by multiprotein nitrogenase complex comprising an Fe protein and a MoFe protein [105]. In the presence of N<sub>2</sub>, oxidized Fe protein reduces by taking electrons from reduced ferredoxin. Reduced Fe oxidizes in the presence of ATP and reduces MoFe protein. MoFe protein donates the electrons to N<sub>2</sub> and reduces it to ammonia in three successive steps: nitrogen to diamine to hydrazine to two ammonia molecules and one H<sub>2</sub>. These reductive steps require electrons from reduced ferredoxins, and their relatively high energy demand makes N<sub>2</sub> fixation unfavorable in *M. maripaludis*. Therefore, cells are less likely to activate this fixation, when ammonia or alanine is available [73, 106].

### Regulation

Cohen-Kupiec et al. [96] hypothesized that both *nif* and *glnA* are regulated by the same nucleotide binding sequences (Fig. 2.5c) residing in the *nif* promoter region of *M. maripaludis*. Lie et al. [107] confirmed this by isolating NrpR protein that represses both N<sub>2</sub> fixation and *glnA* expression by binding to the aforementioned nitrogen operator sequences (*nifOR*). While NrpR represses *nif* transcription fully in the presence of ammonia, it represses partially in the presence of alanine, and depresses fully in the presence of free N<sub>2</sub>. As discussed before, NrpR in turn is regulated by 2-oxoglutarate levels in the TCA cycle [89]. As shown in Fig. 2.5c, the binding of NrpR to *nifOR* weakens during nitrogen deficiency, allowing 2-oxoglutarate to induce *nif* transcription. Experiments have demonstrated that cell

**Table 2.3** A comparison on characteristics of the N<sub>2</sub>-fixing hydrogenotrophs of the order Methanococcales. Modified from [25]

Property	<i>Methanoterris formicicus</i>	<i>Methanococcus maripaludis</i>	<i>Methanococcus aeolicus</i>	<i>Methanothermococcus thermolithotrophicus</i>
Type strain	Mc-S-70	JJ	Nankai-3	SN1
Cell diameter (mm)	0.8–1.5	0.9–1.3	1.5–2.0	1.5
Substrates for methanogenesis	H <sub>2</sub> + CO <sub>2</sub> , formate	H <sub>2</sub> + CO <sub>2</sub> , formate	H <sub>2</sub> + CO <sub>2</sub> , formate	H <sub>2</sub> + CO <sub>2</sub> , formate
Autotrophy	+	+	+	+
Yeast extract stimulates growth	–	+	–	–
Selenium simulates growth	–	+	+	nd
Nitrogen source	NH <sub>3</sub> , N <sub>2</sub> , NO <sub>3</sub>	NH <sub>3</sub> , N <sub>2</sub> , alanine	NH <sub>3</sub> , N <sub>2</sub>	NH <sub>3</sub> , N <sub>2</sub> , NO <sub>3</sub> <sup>–</sup>
Sulfur source	S <sup>2–</sup>	S <sup>2–</sup> , S <sup>0</sup>	S <sup>2–</sup> , S <sup>0</sup>	S <sup>2–</sup> , S <sup>0</sup> , S <sub>2</sub> O <sub>3</sub> <sup>2–</sup> , SO <sub>3</sub> <sup>2–</sup> , SO <sub>4</sub> <sup>2–</sup>
Temperature range (°C)	55–83	<20–45	<20–55	17–70
Temperature optimum (°C)	75	35–40	46	60–65
pH range	6.0–8.5	6.5–8.0	5.5–7.5	4.9–9.8
pH optimum	6.7	6.8–7.2	7	5.1–7.5
NaCl range (% w/v)	0.4–6.0	0.3–5	0.3–6	0.6–9.4
NaCl optimum (% w/v)	2.4	0.6–2	1–2	2–4
Genome size (Mb)	1.82	1.66	1.57	1.69
GC content (mol%)	33	33	32	34
Doubling time (hr)	0.5	2	1.3	~1
Source	Deep-sea black smoker chimney	Salt marsh sediments	Marine sediments	Coastal geothermally heated sea sediments
Reference	[101]	[11]	[100]	[104]

growth with alanine was only marginally lower than that with ammonia, while significantly reduced with free nitrogen [73].

*glnB* proteins play an important role in nitrogen sensing and regulation in *M. maripaludis*. *glnB*<sup>+</sup> strain lost nitrogenase activity within an hour of ammonia addition [108], while *glnB* mutant did not, indicating that these proteins function post-transcriptionally [106]. Kessler et al. [95] also reported the molybdenum dependency of N<sub>2</sub> fixation.

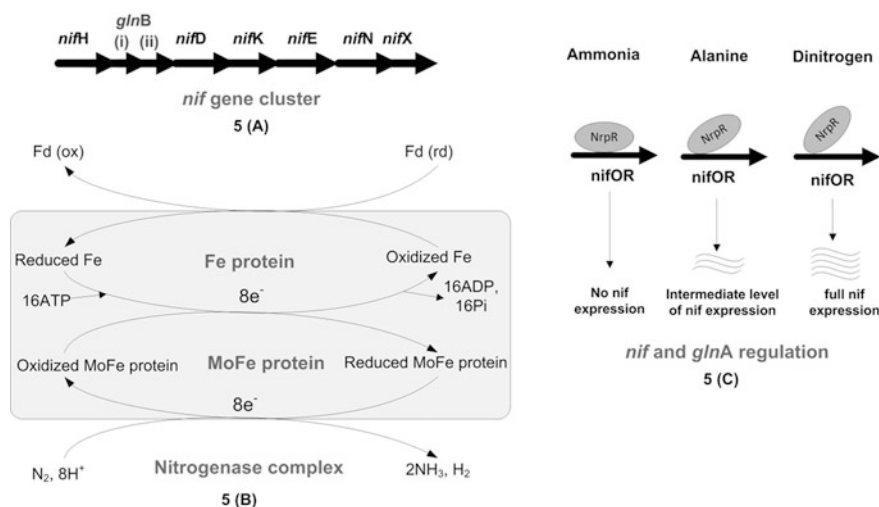


**Fig. 2.5** Nitrogen fixation pathway. **a** The *nif* operon in *M. maripaludis*. **b** Nitrogenase complex. **c** Differential binding of *nif* and *glnA* regulation under different nitrogen substrates/nitrogen limiting conditions. Where, *nifOR* represents *nif* operators

### 2.2.2.8 Amino Acid Metabolism

*M. maripaludis* is an autotrophic organism that synthesizes all amino acids required for its growth. Sequence comparisons of archaeobacterial genes suggest that amino acid biosynthetic enzymes in *Archaea* share a common ancestry with those in *Eubacteria* and *Eukarya* [109]. For instance, the enzymes of branched-chain amino acids (BCAAs) characterized in three methanococci (*M. aeolicus*, *M. maripaludis*, *M. voltae*) were found to be functionally homologous to eubacterial and eukaryotic enzymes with respect to molecular weight, optimum pH, and kinetic properties [109]. Usually, 22 amino acids are required for protein synthesis. 20 amino acids are encoded by the universal genetic codes and the remaining two (selenocysteine and pyrrolysine) are incorporated by unique mechanisms. The 20 amino acids are classified into six groups based on their structures and chemical characteristics of the R group.

In *Methanococcus* spp., the biosynthesis of BCAAs (valine, isoleucine, and leucine) was demonstrated via enzymatic assays [109]. Except *M. voltae* that requires leucine, isoleucine, and acetate for its growth, most species grow autotrophically and possess all the genes and enzymes required for growth. Four enzymes (acetohydroxy acid synthase, acetohydroxy acid isomeroreductase, dihydroxy acid dehydratase, and transaminase B) are required for the syntheses of valine and isoleucine, where 2-ketoisovalerate, an intermediate in valine biosynthesis, acts as a precursor for leucine biosynthesis [109].

The synthesis of alanine occurs from pyruvate via alanine dehydrogenase [72]. Alanine can also serve as the sole nitrogen source during growth [73].

Usually, glycine is synthesized from L-serine via serine hydroxymethyltransferases. *M. thermoautotrophicus* showed the presence of serine hydroxymethyltransferases in the genome [110], but no homologue for this enzyme is present in *M. maripaludis*. Further studies are required to discover the glycine biosynthesis route in methanococci.

The established route of proline biosynthesis involves glutamic acid to proline conversion, but three enzymes of this pathway are absent in most *Archaea* [111]. Graupner et al. [22] demonstrated the synthesis of proline in *M. jannaschii* from cyclization of ornithine via ornithine cyclodeaminase, while no such enzyme has been characterized in *M. maripaludis*, which suggests a possibility of alternate routes.

The biosynthesis of AroAAs (phenylalanine, tyrosine, and tryptophan) is well understood in methanococci. Chorismate acts as the branch point for phenylalanine, tyrosine, and tryptophan synthesis. Unlike *Bacteria*, E4P is not a precursor for chorismate in *M. maripaludis* and an alternate route has been proposed based on the presence of dehydroquinate dehydratase [92]. In this pathway, chorismate is synthesized from 3-dehydroquinate (DHQ) via shikimate pathway. For DHQ synthesis, *M. maripaludis* uses 6-deoxy-5-ketofructose 1-phosphate (DKFP), synthesized after the condensation of methylglyoxal and fructose-1,6-bisphosphate, and L-aspartate-semialdehyde to form 2-amino-3,7-dideoxy-D-threo-hept-6-ulosonate (ADTH), which cyclizes to DHQ [112]. DHQ is not only the precursor for chorismate synthesis, but also acts as a precursor for p-aminobenzoic acid (PABA) synthesis. PABA is an intermediate in *M. maripaludis* during the synthesis of tetrahydromethanopterin, one of the cofactors. [112]. Two biosynthetic routes for the production of AroAAs from chorismate in *M. maripaludis* were proposed previously [92]. To confirm the presence of de novo pathway, deletion strains of MMP1394 encoding 3-dehydroquinate dehydratase were constructed and the mutants were auxotrophic for all three AroAAs and no DHQ activity was detected. To evaluate aryl acid dependent pathway, acids were supplemented to the medium to fulfill the requirements of AroAAs in *M. maripaludis*.

Whole genome sequencing studies on *M. maripaludis* provide information on enzymes/ORFs participating in amino acid biosynthesis. The results indicate that all genes required for the biosynthesis of histidine (*hisA*, B, C, D, E, F, G, H, I) were present in *M. maripaludis* except *hisJ* that encodes for histidinol phosphate phosphatase [22]. Fondi et al. [113] further evaluated the biosynthesis of histidine in *Archaea* and suggested that *his* operon might have been assembled multiple times during evolution because *his* genes scattered throughout the genome. In addition, they showed the existence of *hisN* gene for histidinol phosphate phosphatase and *hisB* gene for imidazoleglycerol-phosphate dehydratase catalyzing sixth and eighth steps of the histidine biosynthesis, which suggests that different molecular mechanisms in *M. maripaludis* may drive piece-wise operon formation for histidine biosynthesis.

Lysine biosynthesis in *M. maripaludis* occurs via diaminopimelate aminotransferase (DapL) pathway [114]. A mutant of *dapL* homolog in *M. maripaludis* resulted in lysine auxotrophy and suggested that *dapL* is essential for lysine biosynthesis.

The specific activities of arginine biosynthetic enzymes in methanogenic *Archaea* was reported by Meile et al. [115]. They also mentioned that although biosynthesis sequences were similar in all microbes, differences existed in reaction steps and regulations of this pathway. Arginine biosynthesis and associated genes/enzymes are well characterized in *M. maripaludis* [22]. The functional conservation of argininosuccinate lyase encoded by *argH* (catalyze final step in arginine biosynthesis pathway) between *M. maripaludis* and the corresponding *Bacteria* and *Eukarya* was demonstrated [116].

Glutamate is synthesized in *M. maripaludis* via glutamate synthase [96]. Aspartate is synthesized by aspartate aminotransferase and asparagine glutamine-hydrolyzing asparagine synthase (*asnB*). <sup>14</sup>C labeling studies on *M. barkeri* and other *Archaea* showed that synthesis of alanine, aspartate, and glutamate occurred from pyruvate, oxaloacetate, and  $\alpha$ -ketoglutarate respectively [117].

<sup>13</sup>C labeling of serine was consistent with its synthesis from pyruvate via 3-phosphoglycerate. *M. maripaludis* contained *serA* and *serB*, but not a homolog for *serC* [22]. Similarly, a homolog for glycine hydroxymethyltransferase encoded by *glyA* is absent for synthesis of glycine from serine.

Stathopoulos et al. [118] challenged the notion that all 20 aminoacyl-tRNA synthetases are essential for the viability of a cell. They knocked out *cysS* gene encoding cysteinyl-tRNA synthetase (CysRS) from *M. maripaludis* and showed that pure *M. maripaludis* prolyl-tRNA synthetase (ProRS) can form cysteinyl-tRNA (Cys-tRNA), implying dual-specificity of enzyme for the loss of CysRS. The report by Stathopoulos et al. [118] was incorrect. While ProRS has low levels of CysRS activity, it is not physiologically significant. Sauerwald et al. [119] demonstrated this by observing that CysRS mutants could not incorporate exogenous cysteine into cellular protein. The tRNA-dependent cysteine biosynthesis pathway in *M. maripaludis* is well established and occurs in two steps: First, O-phosphoseryl-tRNA ligase (SepRS) aminoacylates uncharged Cys-tRNA with 3-phospho-L-serine (Sep) to form O-phosphoseryl-tRNA (Sep-tRNA). Second, Sep-tRNA:Cys-tRNA synthase (SepCysS) transforms Sep to cysteine [119]. Zhang et al. [120] showed that these two enzymes (SepRS and SepCysS) form a stable binary complex and promote the conversion of intermediate Sep-tRNA to cysteinyl-tRNA by sequestering the binding of the intermediate to elongation factor EF-1 $\alpha$  or infiltrating into the ribosome.

Methionine biosynthesis in *M. maripaludis* is unclear. Only one ORF, MMP0401, has been identified in *M. maripaludis* via sequencing studies [22] which indicates the synthesis of methionine from homocysteine. The presence of cystathionine  $\beta$ -lyase (*metC*) in *M. maripaludis* indicates the possibility that *M. maripaludis* synthesizes homocysteine (the intermediate precursor of methionine) either by transsulfuration route with cystathione or via direct sulfhydrylation of O-acetylhomoserine [114]. Such gaps in the literature need further investigation of existing routes or novel biosynthetic routes.



Selenocysteine is the selenium containing 21st amino acid that is co-translationally incorporated into proteins, which are known as selenoproteins. The amino acid is coded by UGA, which is normally a termination codon during protein synthesis. Only 20 % of *Bacteria* and 10 % of *Archaea* (*Methanococcus*, *Methanocaldococcus*, and *Methanopyrus* spp.) were found to have machinery for Sec insertion. In *Eukarya*, sec insertion machinery is common in lower organisms, such as green algae and moulds [121]. Yuan et al. [122] proposed tRNA<sup>Sec</sup>-dependent conversion of *O*-phosphoserine (Sep) to selenocysteine in *Eukarya* and *Archaea*. Genetic analysis of selenocysteine biosynthesis in *M. maripaludis* is reported in the literature [123–125].

Pyrrolysine is the 22nd natural amino acid and is a lysine derivative encoded by UAG. It is used by methanogenic *Archaea* and was discovered in 2002 at the active site of methylamine methyltransferase in *M. barkeri* [126]. *pylT* gene, whose tRNA product has CUA anticodon, translates to UAG codon as pyrrolysine in some methanogens. The presence of pyrrolysine in *M. maripaludis* is not established, although it has been mentioned in non-pyl-utilizing *Archaea* in the literature [127].

### 2.2.2.9 Nucleotide Biosynthesis

Nucleotides include purines (adenine and guanine) and pyrimidines (thymine and cytosine). In RNA, adenine base pairs with uracil instead of thymine. The purine and pyrimidine biosynthesis in *M. maripaludis* is very well understood and sequencing study showed the presence of related genes involved in biosynthesis of purines and pyrimidines [22]. 5-phospho- $\alpha$ -D-ribose 1-diphosphate (PRPP) is synthesized from ribose-5-phosphate with the help of PRPP synthetase and combines with glutamine to form 5-phosphoribosylamine, which goes through a series of reactions and forms inosinic acid (IMP). IMP acts as the branch point for adenosine monophosphate (AMP) and guanosine monophosphate (GMP) biosynthesis in the pathway. AMP is synthesized from IMP and adenylosuccinate and converted to other purine nucleotides, such as adenosine diphosphate (ADP) and adenosine triphosphate (ATP). Similarly, xanthosine 5'-monophosphate (XMP) is synthesized from IMP with NAD<sup>+</sup> or NADP<sup>+</sup> as acceptors, which is subsequently converted to other purine nucleotides, such as GMP, guanosine diphosphate (GDP), and guanosine triphosphate (GTP). Pyrimidine biosynthesis converts bicarbonate, L-glutamine, orotate, and PRPP, to uridine monophosphate (UMP) for further conversion to uridine triphosphate (UTP) and cytidine triphosphate (CTP) for participation in nucleic acid biosynthesis.

### 2.2.3 Molecular Biology Tools

*M. maripaludis* is a well-studied model organism. The 1.6 Mb long *M. maripaludis* genome covers 1722 protein-coding genes and is exceptional in the presence of



unique hydrogenases [53]. Genetic maps are available to help identify the functions of ORFs across methanogens [22, 128, 129]. A set of genetic tools is available for the manipulation of its fully sequenced genome via selectable markers [130], shuttle vectors [131], integrative plasmids and gene replacements [132], and markerless mutagenesis [72].

### 2.2.3.1 Selectable Markers

It is very difficult to identify antibiotic resistant markers in methanogens due to the absence of peptidoglycans in their cell walls and different ribosome structures. Puromycin resistance in *M. maripaludis* was reported by transforming it with pKAS100 and pKAS102 plasmids [131]. To complement the method of vector transformation, an optimized polyethylene glycol (PEG) method of transformation was used [133]. With the PEG method, transformation frequency increased four to five orders of magnitude ( $2 \times 10^5$  transformants/ $\mu\text{g}$  of insertion vector) than with the natural transformation method. Methylation of plasmid with PstI methylase increased the transformation efficiency by at-least four-folds, approaching those obtained for *Escherichia coli* (*E. coli*) and addition of divalent cations inhibit the transformation [133]. Neomycin is the second selectable marker reported previously [130]. Aminoglycoside phosphotransferase genes APH3'I and APH3'II cloned under the control of *Methanococcus voltae* methyl reductase promoter can act as a neomycin resistance marker in *M. maripaludis* [130]. The MIC of neomycin to completely inhibit 5 ml culture of *M. maripaludis* growth was determined to be 1000  $\mu\text{g}/\text{ml}$ . Concentration between 500 and 1000  $\mu\text{g}/\text{ml}$  delayed its growth. Kanamycin and geneticin are non-inhibitory for *M. maripaludis* cells [134, 135].

### 2.2.3.2 Shuttle Vectors

Shuttle vector pDLT44 was constructed for *M. maripaludis* JJ using plasmid pURB500 (from *M. maripaludis* C5) and pMEB.2, (*E. coli* vector containing a methanococcal puromycin resistance marker) [136]. The shuttle vector was found to be stable in *E. coli* under ampicillin selection. This was the first report of a plasmid replicated independently in a methanogen and can be manipulated in *E. coli*. Although pURB500 was originated from a methanococcus, it did not replicate in *M. voltae*. In another study, development of expression shuttle and integrative vector for *M. maripaludis* has been reported to use histone promoter ( $P_{hmvA}$ ) and multiple cloning sites from *M. voltae* for overexpression of *ilvBN* and *ppsA* [137]. These expression vectors may be useful for studying the physiology and biochemistry of *M. maripaludis*. The transformation efficiency may vary from one strain to another [138]. *M. maripaludis* S2 did not show the same high level of transformation as reported for *M. maripaludis* JJ. Therefore, transformation rates were improved by manipulating the shuttle vector. Walters et al. [138] showed that a significantly smaller shuttle vector pAW42 was sufficient to maintain in

*M. maripaludis* S2 and provides 7000-fold increase in transformation efficiency for pURB500-based vectors.

### 2.2.3.3 Integrative Plasmid and Gene Replacement

Integration vector pIJA03-cysS for *M. maripaludis* was constructed to determine the essentiality of *cysS* gene coding for cysteinyl-tRNA synthetase [118]. In the same study, *cysS* gene replacement was carried out by constructing a pBD1 vector by using the plasmid pPH21310. Several other mutants of *M. maripaludis* have been constructed using the technique of integrative plasmids and gene replacement. For example, acetate auxotrophs were isolated by random insertional mutagenesis by transforming the wild type *M. maripaludis* with pWDK104 [139]. Using transposon insertion mutagenesis, mutations were made in and around *nifH* gene and nitrogen fixing abilities of four transformants were studied. In another study of transposon insertion mutagenesis, an 8-kb region corresponding to the *nif* gene cluster was confirmed for N<sub>2</sub>-fixation [103].

### 2.2.3.4 Markerless Mutagenesis

To demonstrate the role of genes that show unusual ability to use D-alanine or L-alanine, markerless mutagenesis in *M. maripaludis* was demonstrated [72]. They used a negative selection based system that used *hpt* and *upt* gene encoding hypoxanthine phosphoribosyltransferase and uracil phosphoribosyltransferase present in *M. maripaludis*. Hpt system was used to produce markerless in-frame deletion mutation in three genes (*ald*, *alr*, and *agcS*) coding for alanine dehydrogenase, alanine racemase, and alanine permease. *Hpt* was used together with *upt* to restore the function of wild type *ald* [72].

## 2.2.4 Potential Applications

Methanogens play a key role in the global carbon cycle by reducing atmospheric CO<sub>2</sub> [55]. The unique characteristics of *M. maripaludis* in particular, and methanogens in general, offer the potential for several industrial and environmental applications such as wastewater treatment, carbon capture and utilization, and methane from renewable energy via electro-methanogenesis.

### 2.2.4.1 Wastewater Treatment

Tabatabaei et al. [140] has summarized the characteristics of methanogenic populations used in wastewater treatment. The production of biogas from waste relies on

a symbiotic relationship between syntrophic bacteria (*Syntrophomas*, *Syntrophospora*, and *Syntrophobacter*) and methanogens [141]. Syntrophic acetogenic bacteria convert acid-phase products into acetates and H<sub>2</sub>, which are then utilized by methanogenic archaea. If accumulated H<sub>2</sub> is not used by the methanogens, then acetogenesis during anaerobic degradation cannot occur [142]. That is where *M. maripaludis* has a potential to play a key role in maintaining a low partial pressure of H<sub>2</sub> by consuming it rapidly.

In a biogas plant, the actual proportions of acetoclastic and hydrogenotrophic methanogens may depend on the conditions [143]. It has been frequently seen that hydrogenotrophic methanogens dominate at high temperatures (>50 °C). This is primarily because hydrogenotrophic methanogens can degrade acetate with syntrophic bacteria more efficiently at high temperatures than acetoclastic methanogens.

New evidence also suggests that direct electron transfer through nanowires/ electrically conductive pili may also be present between bacteria and these methanogens during anaerobic digestion [144–146].

### 2.2.4.2 Carbon Capture and Conversion

Flue gas exhausts from power plants typically have 3–15 % CO<sub>2</sub> in majority N<sub>2</sub>. These CO<sub>2</sub> emissions are the major contributors to global warming and climate change [147]. Reducing CO<sub>2</sub> emissions by capturing and sequestering or converting the CO<sub>2</sub> to fuels and value-added chemicals is an area of active research around the globe. *M. maripaludis* with its ability to uptake CO<sub>2</sub> in the presence of N<sub>2</sub> offers an attractive route to capture and convert CO<sub>2</sub> simultaneously from flue gas emissions to useful fuels such as methane and methanol [108]. In combination with other methanogens such as *M. aeolicus* [100], *M. thermolithotrophicus* [99], *M. formicicus* [101], it is possible to utilize microbe consortia to reduce carbon emissions from power and chemical plants on a large scale, and alleviate environmental and global warming concerns.

### 2.2.4.3 Methane from Renewable Energy

The main challenge in using methanogens for large-scale biomethane production is the need for H<sub>2</sub>. The only viable source for this H<sub>2</sub> is renewable energy sources such as solar, tidal, and wind. The transient nature of these resources raises the need for temporary storage of energy in a stable chemical form. One possibility is to convert surplus renewable electricity directly into methane via electrochemical methanogenesis. This is already established for a mixed-culture of methanogenic microbes comprising *Methanobacterium* sp. (>93 %) and *Methanobrevibacter* (~5 %) [148]. Recently, Lohner et al. [45] has also demonstrated the uptake of electrons by a hydrogenase-mutant of *M. maripaludis*. However, methane

production relative to the wild type was only 1/10 as discussed before. These studies show that methanogens can be used as biocatalysts for electrochemical conversion of CO<sub>2</sub>.

Another alternative is to use surplus renewable electricity for non-microbial electrochemical conversion of CO<sub>2</sub> to formate [149] and then convert formate into methane using *M. maripaludis*.

#### 2.2.4.4 Hydrogen Production

H<sub>2</sub> production by various aerobic and anaerobic microbes has been reported in the literature [150, 151]. The highest rates reported for genetically engineered *E. coli* strains ranges from 1.7  $\mu\text{mol/mg DCW.min}$  to 4.2  $\mu\text{mol/mg DCW.min}$  [152] from formate. The methylotrophs *Methylomonas albus* and *Methylosinus trichosporium* showed H<sub>2</sub> production rates of 1.6 and 0.4  $\text{nmol/mgDCW.min}$  respectively from formate [153]. However, the rates reported by wild-type formate-grown *M. maripaludis* S2 are much higher i.e. 1.4  $\mu\text{mol/mg DCW.min}$  [42].

#### 2.2.4.5 Other Applications

Several applications remain unexplored for *M. maripaludis* in spite of its unique advantages such as rapid growth, ease of genetic manipulation, fully sequenced genome, and available genome-scale model. For instance, *M. maripaludis* can potentially be used to produce high value-added pharmaceuticals, vitamins, amino acids, corrinoids, and terpenoids, and these possibilities require further research. An excellent example is geraniol, a useful flavoring agent [154], which can be produced by genetically engineered *M. maripaludis*. Biotransformation of 2,4,5-trinitrotoluene, a priority pollutant, and metabolic conversion of 5-methylfurfurals and 2-methylfufurals (formed during the concentration of aqueous wastes in paper and pulp industries) to furfurals have been studied with *Methanococcus spp.* (strain B) [155, 156]. Such biotransformations can also be explored with *M. maripaludis*. Other possible applications could be the production of liquid biofuels such as methanol, butanol, etc.

### 2.3 Genome-Scale Engineering

The concept of metabolic pathway manipulation for purpose of using microorganisms with desirable properties is quite old. The methods for identifying superior strains rely heavily on the use of chemical mutagens and creative selection techniques [157]. Despite its success, the genetic and metabolic profiles of these mutant strains are poorly characterized. Recombinant DNA technology (rDNA) introduced a new dimension to the work and genetic modification of enzymatic reactions

allowed precise modifications in metabolic pathways [158]. After the feasibility of rDNA technology, various terms were coined to represent the potential applications of this technology, namely molecular breeding [159], in vitro evolution [158], pathway engineering [160], cellular engineering [160], and metabolic engineering [161]. All convey similar meaning and defined as “directed improvement of product formation or cellular properties through the modification of specific biochemical reaction(s)”. Instead of ad hoc target selection process, a rational process to identify the most promising target for metabolic manipulation would save experimental efforts. Therefore, we are witnessing a paradigm shift away from individual enzymatic reactions.

Metabolic engineering focuses on integrated metabolic pathways instead of individual reactions and shifted our attention to the complete biochemical reaction networks instead of its constituent parts. It examines issues of pathway synthesis, thermodynamic feasibility, and pathway flux and its control [161]. Observations about the behavior of overall system provide the best guide for rational analysis. Metabolic engineering needs to be complemented with the appropriate measurements to achieve maximum results. Specific areas of industrial production where metabolic engineering can make significant impact are the production of petroleum-derived thermoplastics by fermentation, biologically active agents such as polyketides, amino acid production, vitamins, organic acids, lipid, oil and a list of other product classes [162–165]. In addition to manufacturing, it can have significant impact on medical field such as identifying targets for drug development [166].

### **2.3.1 Systems Biology Models: Kinetic Versus Stoichiometric**

In silico mathematical models can be classified as either kinetic or stoichiometric. Kinetic models describe the dynamic behavior of a cell. They involve temporal ordinary differential equations describing the concentration profiles of metabolites based on rate laws postulated for key metabolic reactions. While kinetic models are simple to construct, they face serious limitations. Firstly, they involve numerous model parameters such as rate constants, which are difficult to measure or even estimate reliably. In most cases, the dynamic data on metabolite concentration profiles is insufficient to fit reliable values for these parameters. Secondly, kinetic models become highly unwieldy and complex, when applied at the genome level. Therefore, most kinetic models are for either subsystems or simplified through appropriate assumptions. Several kinetic models have been developed to understand the effects of metabolic perturbations in subsystems. Some examples are glycolysis in plant tubers [167], mitochondrial respirations [168], calvin cycle [169], microbial growth kinetics during fermentation [170, 171], anaerobic glycolysis of yeast *Saccharomyces cerevisiae* [172], glycogenolysis in mammalian FT skeletal muscle [173], and salicylamide (SAM) metabolism in the perfused rat liver [174] etc.

Stoichiometric models, on the other hand, are inherently non-dynamic and rely on reaction stoichiometry alone. Their main assumption is that the internal metabolites are at pseudo-equilibrium. When such metabolic models are developed based on genome sequence and Gene-Protein-Reaction (GPR) associations, they are called genome-scale metabolic models or constraint-based flux models. Since the first genome-scale metabolic model was constructed for *Haemophilus influenzae* [175], many such models have been constructed for a variety of organisms and experimentally validated. The success rate of in silico predictions is typically about 70–90 % depending on the types of organism and prediction [176]. The constraints in the model is the underlying main concept that separate feasible and infeasible metabolic behavior and are much easier to identify than kinetic parameters, making large scale model building possible [177]. Three main constraints that need to be satisfied by a model are: Firstly, *Physicochemical constraints* defined by conservation laws of mass and energy, dependency of reaction rates on metabolite concentrations, and negative free energy change for spontaneous reactions. Secondly, *Environmental constraints* such as availability of nutrients or electron acceptors etc. imposed as result of specific conditions. Lastly, *Regulatory constraints* i.e. up-regulated/down-regulated gene expressions as the cell undergo environmental perturbations.

In this thesis, we develop a genome-scale metabolic model based on stoichiometric constraint-based approach to predict the behavior of complex biological interactions via FBA. When FBA is applied for the determination of metabolic pathway fluxes, the approach is renamed as Metabolic Flux Analysis (MFA).

### 2.3.1.1 Constraints-Based Modeling

#### Drafting a metabolic network

It is a process during which various components of the cellular metabolic pathways e.g. associated genes, proteins, reactions and metabolites are identified through various online databases (KEGG, BioCyc, etc.), genome-wide annotations, published literature, etc. and categorized to form a network [178]. Online resources that are helpful for drafting a metabolic network are extensively reviewed in literature [179]. A number of automated systems to help us in genomics data analysis are also available such as GeneQuiz, Pedant, Magpie, etc. [180]. The reconstructed network or a draft model generated from the well-annotated reactions acts as the starting point of genome-scale modeling. The draft models are manually refined by incorporating genetic, biochemical and functional information before converting into a mathematical model.

#### Metabolic Flux Analysis (MFA)

MFA is a powerful approach for the determination of metabolic pathway fluxes, whereby intracellular fluxes are calculated using stoichiometric matrix of the reactions and applying mass balance on intracellular metabolites [179]. The metabolic

network is represented in the form of a stoichiometric matrix  $S$ , where row represent is the number of metabolites and  $n$  is the number of reactions/fluxes occurring in a organism.  $S_{ij}$ , the element of a stoichiometric matrix  $S$ , corresponds to metabolite  $i$  and reaction  $j$ . The static models assume a pseudo steady state and transient mass balance represented as follows:

$$\frac{dX}{dt} = S.v - b = 0 \quad (2.1)$$

Here  $S$  is the  $i \times j$  stoichiometric matrix,  $v$  is the vector of  $n$  metabolic reactions and  $b$  is the vector of net known metabolite uptake by the cell.

Typically Eq. 2.1 represents an underdetermined system ( $j > i$ ) and hence an infinite solution exists with a number of cell phenotypes. To obtain a particular solution, a linear optimization is formulated in which one can find a flux distribution that minimizes or maximizes a particular objective  $Z$ . A number of different objective functions have been reviewed in literature such as minimize energy, minimize nutrient uptake, minimize redox production, minimize the Euclidean norm and maximize metabolite production [181, 182]. The most commonly used objective function is maximizing biomass [183]. The mathematical formulation is

$$\text{Maximize } Z = \sum_{j=1}^j c_j v_j \text{ subject to } S.v = b \quad (2.2)$$

where,  $Z$  is the cellular objective that is represented as a weighted sum of metabolite fluxes  $v_j (j = 1, 2, \dots, j)$  with weights  $c_j$ .

The final metabolic flux map shows the estimation of steady-state rate (flux) for all the essential reactions contributing to our objective function. A metabolic flux map contains useful information about the contribution of various pathways towards substrate utilization and product formation. Genetic and environmental perturbations in the system help us to compare specific pathways and reactions in different situations. In addition to quantitative pathway fluxes, MFA provides insights about cell physiological characteristics. Some of them are listed here:

- Identification of branch point control (nodal rigidity)
- Identification of alternate pathways: e.g. transhydrogenase activity in *C. glutamicum* [184]
- Calculation of non-measured extracellular fluxes
- Calculation of maximum theoretical yields.

### 2.3.1.2 Simulation Tools

Theoretically, MFA is well understood and simple however it is not easy for researchers to manually implement MFA without computational coding and basic

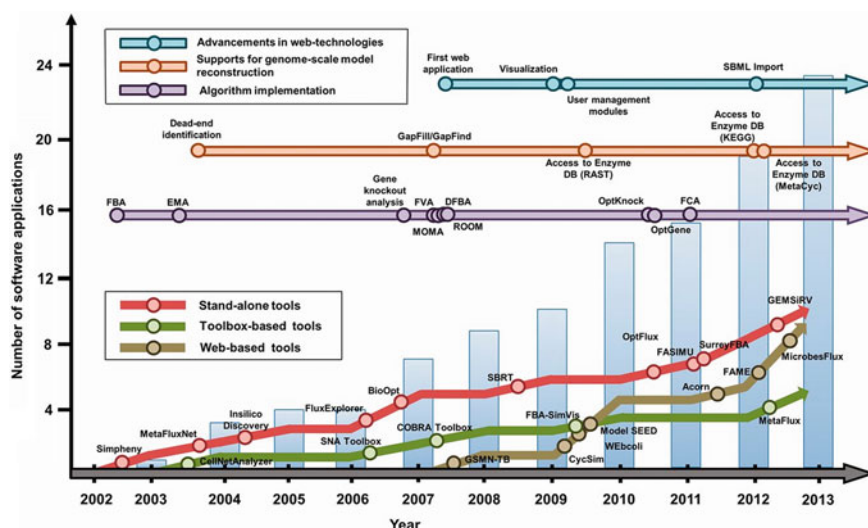


**Fig. 2.6** Timeline of FBA software tools developed over a past few years as reported by Lakshmanan et al. [185]

programming skills because of the large number of reactions and metabolites present in an organism. To quantify metabolic fluxes across the pathway, FBA tools have been developed and are freely available online [185]. These tools aid in model development and FBA. They have been divided into three major types. Stand-alone, toolbox-based, and web-based applications as shown in Fig. 2.6 [185]. Some of the most commonly used applications are Simpheny, MetaFluxNet, BioOpt, OptFlux, GEMSiRV, and COBRA Toolbox. Each of these tools is associated with some unique features and limitations.

### 2.3.1.3 Applications

Genome-scale models are very useful in understanding the interaction of intracellular host functions and the impact of various genetic perturbations on cell behavior. They have been successfully used for fruitful results in many applications. Some examples are (i) Enhanced metabolite production e.g. Butanol production by *Clostridium acetobutylicum* [186], L-lysine production by *Corynebacterium spp.* [187] etc. (ii) Production of new metabolites which are not secreted by microbes such as indigo production by *E. coli* [188], polyhydroxyalkanoate production by *E. coli* [189], etc. (iii) Effect of different media components on cell growth and product formation e.g. effect of various carbon and nitrogen sources on desulfurization activity of *Rhodococcus erythropolis* [190], L-tryptophan production from



sucrose in *E. coli* [191], ethanol production from starch by *Saccharomyces cerevisiae* [192], etc. (iv) Design of new/improved metabolic pathways for degradation of various chemicals e.g. degradation of mixture of xylene, toluene and benzene by *Pseudomonas putida* [193], degradation of chloro-organic compounds by *Dehalococcoides* spp. [194] for bioremediation (v) Modification of cell properties to facilitate bioprocessing e.g. better growth of *E. coli* and other microbes under microaerobic conditions [195], slow growth rate and high methane flux under nitrogen gas as the sole nitrogen source [196], ammonia transport without ATP consumption in *Methylophilus methylotrophus* [197], etc. (vi) Understanding the symbiotic relationships e.g. symbiotic relationship of *Rhizobium etli* with plants [198], mutualistic interactions between methanogen *M. maripaludis* and sulfate-reducing bacteria *Desulfovibrio vulgaris* [199] etc.

### 2.3.2 iMM518: A Genome-Scale Model

In recent years, systems biology models have been widely used to understand, analyze, and quantify the extent and impact of complex biological interactions and genetic perturbations [200]. Goyal et al. [201] reported the first constraint-based genome-scale metabolic model (iMM518) for *M. maripaludis*. The model includes 570 reactions, 556 metabolites, and 518 genes across 52 pathways. They identified essential and non-essential genes/reactions, and compared the effectiveness of various carbon, hydrogen, and nitrogen sources. Their analyses confirmed that methane production and cell growth compete with each other for available carbon as expected, and methane flux can only be increased at the expense of growth. Sarmiento et al. [202] analyzed gene functions in *M. maripaludis* using whole-genome libraries of Tn5 transposon mutant. While they considered all genes, iMM518 focused only on the 30 % of ORFs involved in metabolism. It is interesting that 34 metabolic genes deemed essential for growth by Sarmiento et al. [202] were also deemed essential by iMM518. Goyal et al. [201] also identified the best gene combinations whose deletions would maximize methane production rate. Some of their identified targets for single and multiple gene deletions are *adkA* (MMP1031), *acd* (MMP0253), *mdh* (MMP0645), *acd* (MMP0253) and *mdh* (MMP0645), *adkA* (MMP1031) and *mdh* (MMP0645), and *acd* (MMP0253) and *cimA* (MMP1018) and *mdh* (MMP0645). The details of the reactions and enzymes are available in [201].

Using iMM518, Goyal et al. showed that N<sub>2</sub> fixation enhances MERs by 7.84 % and reduces growth rate by approx. 50 % compared to NH<sub>3</sub> [201]. Thus, free N<sub>2</sub> is better for methane production than ammonia and in reducing production of waste biomass. We confirmed the same with our ongoing experiments (unpublished). A comparison of *M. maripaludis* S2 with *M. barkeri* and *M. acetivorans* showed *M. maripaludis* to be a better methanogen for producing methane.

## 2.4 Microbial Electrolysis Cells (MECs)

Recent years have been a turning point for research in microbial bioelectrochemical processes, i.e. whole cell microorganisms are used to catalyze oxidation and/or reduction reactions [203]. Microbial Fuel Cells (MFCs) are one of the examples, which harness electric current from microbes [204]. Another context is MECs, a reverse of MFCs, where applied potential is used to carry out microbial metabolism and biochemical production. This process is known as microbial electrosynthesis [205]. Microbes take external electrons from electrical inputs and reduce carbon source to useful chemicals with the help of hydrogen ions produced during water splitting. Some of the examples are production of acetate from  $\text{CO}_2$  [206], fumarate to succinate conversion [207], and increased glutamate yield from glucose fermentation [208].

Electromethanogenesis by archaeon, *Methanobacterium palustre* was demonstrated by Cheng et al. [209]. A recent study on *Sporomusa ovata* by Nevin et al. [206] showed that microbiological catalysts might be a robust alternative for converting  $\text{CO}_2$  and water to multi-carbon extracellular compounds, when coupled with photovoltaics. They further extended the work to wider range of microorganisms including two other *Sporomusa* species, *Clostridium ljungdahlii*, *Clostridium acetivum*, and *Moorella thermoacetica* and showed production of organic acids mainly acetate [210]. Some of the major achievements towards microbial electrosynthesis are shown in Fig. 2.7. One of the means of cathodic extracellular electron transfer is through hydrogen [211]. This gas can readily be produced at cathodes and serve as driver for microbial metabolism without affecting microbial integrity. This fact along with range of products formed during metabolism driven by  $\text{H}_2$  makes first stepping stone towards electricity driven bio-production of chemicals such as methane.

Lohner et al. [212] demonstrated electromethanogenesis i.e.  $\text{H}_2$ -independent growth via a hydrogenase-deficient strain of *M. maripaludis*. However methane

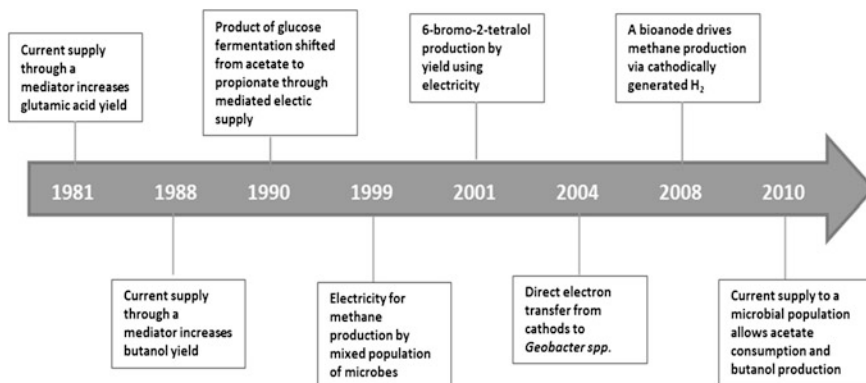


Fig. 2.7 History of major achievements towards microbial electrosynthesis [211]

production rates reduced to 1/10 of that in wild-type cells. They used two chamber (anode and cathode) borosilicate gastight chamber and a Nafion 117 proton exchange membrane separating both the chambers.

Substantial pH gradient between the anode and the cathode contribute to potential losses [213]. Membranes in two chamber setups increases ohmic resistance of the cell result in lower current production for an applied cell potential [31]. In addition, membranes are very expensive. These issues can be avoided with a membraneless reactors [214]. In this thesis, we developed a single-chamber membrane-free MEC for demonstration of electromethanogenesis by a pure culture of wild type *M. maripaludis* S2 and reported preliminary results.

## References

1. Saini R, Kapoor R, Kumar R, Siddiqi TO, Kumar A (2011) CO<sub>2</sub> utilizing microbes—a comprehensive review. *Biotechnol Adv* 29:949–960
2. Wood HG, Werkman C (1940) The fixation of CO<sub>2</sub> by cell suspensions of *Propionibacterium pentosaceum*. *Biochem J* 34:7–14
3. Werkman CH, Wood HG (2009) Heterotrophic assimilation of carbon dioxide. *Adv Enzymol Relat Areas Mol Biol. Part B: Mechanism of Enzyme Action*, 74(227):3
4. Thauer RK (2007) A fifth pathway of carbon fixation. *Science* 318:1732–1733
5. Evans M, Buchanan BB, Arnon DI (1966) A new ferredoxin-dependent carbon reduction cycle in a photosynthetic bacterium. *Proc Natl Acad Sci USA* 55:928
6. Wood HG (1991) Life with CO or CO<sub>2</sub> and H<sub>2</sub> as a source of carbon and energy. *FASEB J* 5:156–163
7. Herter S, Fuchs G, Bacher A, Eisenreich W (2002) A bicyclic autotrophic CO<sub>2</sub> fixation pathway in *Chloroflexus aurantiacus*. *J Biol Chem* 277:20277–20283
8. Berg IA, Kockelkorn D, Buckel W, Fuchs G (2007) A 3-hydroxypropionate/4-hydroxybutyrate autotrophic carbon dioxide assimilation pathway in Archaea. *Science* 318:1782–1786
9. Huber H, Gallenberger M, Jahn U, Eylert E, Berg IA, Kockelkorn D, Eisenreich W, Fuchs G (2008) A dicarboxylate/4-hydroxybutyrate autotrophic carbon assimilation cycle in the hyperthermophilic Archaeum *Ignicoccus hospitalis*. *Proc Natl Acad Sci* 105:7851–7856
10. Wang B, Li Y, Wu N, Lan CQ (2008) CO<sub>2</sub> bio-mitigation using microalgae. *Appl Microbiol Biotechnol* 79:707–718
11. Jones WJ, Paynter MJB, Gupta R (1983) Characterization of *Methanococcus maripaludis* sp. nov., a new methanogen isolated from salt marsh sediment. *Arch Microbiol* 135:91–97
12. Keswani J, Orkand S, Premachandran U, Mandelco L, Franklin M, Whitman W (1996) Phylogeny and taxonomy of mesophilic *Methanococcus* spp. and comparison of rRNA, DNA hybridization, and phenotypic methods. *Int J Syst Bacteriol* 46:727–735
13. Whitman WB, Shieh J, Sohn S, Caras DS, Premachandran U (1986) Isolation and characterization of 22 mesophilic methanococci. *Syst Appl Microbiol* 7:235–240
14. Escalante-Semerena J, Rinehart K, Wolfe R (1984) Tetrahydromethanopterin, a carbon carrier in methanogenesis. *J Biol Chem* 259:9447–9455
15. Zellner G, Winter J (1987) Secondary alcohols as hydrogen donors for CO<sub>2</sub> reduction by methanogens. *FEMS Microbiol Lett* 44:323–328
16. Shieh J, Whitman WB (1988) Autotrophic acetyl coenzyme A biosynthesis in *Methanococcus maripaludis*. *J Bacteriol* 170:3072–3079

17. Costa KC, Yoon SH, Pan M, Burn JA, Baliga NS, Leigh JA (2013) Effects of H<sub>2</sub> and formate on growth yield and regulation of methanogenesis in *Methanococcus maripaludis*. J Bacteriol 195:1456–1462
18. Liu Y (2010) Methanococcales. In: Handbook of hydrocarbon and lipid microbiology. Springer, Berlin, pp 573–581
19. Copeland A, Lucas S, Lapidus A, Barry K, Glavina del Rio T, Dalin E, Tice H, Pitluck S, Chertkov O, Brettin T, Bruce D, Han C, Detter JC, Schmutz J, Larimer F, Land M, Hauser L, Kyrpides N, Mikhailova N, Sieprawaska-Lupa M, Whitman WB, Richardson P (2007) Complete genome sequence of *Methanococcus maripaludis*. Unpublished: US DOE Joint Genome Institute
20. Mori K, Tsurumaru H, Harayama S (2010) Iron corrosion activity of anaerobic hydrogen-consuming microorganisms isolated from oil facilities. J Biosci Bioeng 110:426–430
21. Wang X, Greenfield P, Li D, Hendry P, Volk H, Sutherland TD (2011) Complete genome sequence of a nonculturable *Methanococcus maripaludis* strain extracted in a metagenomic survey of petroleum reservoir fluids. J Bacteriol 193:5595
22. Hendrickson EL, Kaul R, Zhou Y, Bovee D, Chapman P, Chung J, Conway de Macario E, Dodsworth JA, Gillett W, Graham DE et al (2004) Complete genome sequence of the genetically tractable hydrogenotrophic methanogen *Methanococcus maripaludis*. J Bacteriol 186:6956–6969
23. Liu Y, Whitman WB (2008) Metabolic, phylogenetic, and ecological diversity of the methanogenic archaea. Ann N Y Acad Sci 1125:171–189
24. Ferry JG (1994) Bioenergetics of methanogenesis. In: Ferry JG (ed) Methanogenesis—ecology, physiology, biochemistry & genetics. Chapman and Hall, New York, p 536
25. Whitman W, Jeanthon C (2006) Methanococcales. In The prokaryotes. Springer, New York, pp 257–273
26. Koga Y, Morii H, Akagawa-Matsushita M, OHGA M (1998) Correlation of polar lipid composition with 16S rRNA phylogeny in methanogens. Further analysis of lipid component parts. Biosci Biotechnol Biochem 62:230–236
27. Dworkin M, Falkow S (2006) The prokaryotes, vol 3. Archaea. bacteria: firmicutes, actinomycetes. Springer, Berlin
28. Akca E, Claus H, Schultz N, Karbach G, Schlott B, Debaerdemaeker T, Declercq JP, Konig H (2002) Genes and derived amino acid sequences of S-layer proteins from mesophilic, thermophilic, and extremely thermophilic methanococci. Extremophiles 6:351–358
29. Jones W, Donnelly M, Wolfe R (1985) Evidence of a common pathway of carbon dioxide reduction to methane in methanogens. J Bacteriol 163:126–131
30. Hedrick DB, Guckert J, White D (1991) Archaeobacterial ether lipid diversity analyzed by supercritical fluid chromatography: integration with a bacterial lipid protocol. J Lipid Res 32:659–666
31. Jarrell KF, Koval SF (1989) Ultrastructure and biochemistry of *Methanococcus voltae*. Crit Rev Microbiol 17:53–87
32. Jarrell KF, Jones GM, Kandiba L, Nair DB, Eichler J (2010) S-layer glycoproteins and flagellins: reporters of archaeal posttranslational modifications. Archaea 2010:13
33. Jarrell KF, Stark M, Nair DB, Chong JP (2011) Flagella and pili are both necessary for efficient attachment of *Methanococcus maripaludis* to surfaces. FEMS Microbiol Lett 319:44–50
34. Bardy SL, Jarrell KF (2002) FlaK of the archaeon *Methanococcus maripaludis* possesses preflagellin peptidase activity. FEMS Microbiol Lett 208:53–59
35. Chaban B, Ng SY, Kanbe M, Saltzman I, Nimmo G, Aizawa S, Jarrell KF (2007) Systematic deletion analyses of the *fla* genes in the flagella operon identify several genes essential for proper assembly and function of flagella in the archaeon, *Methanococcus maripaludis*. Mol Microbiol 66:596–609

36. Thomas NA, Mueller S, Klein A, Jarrell KF (2002) Mutants in *flaI* and *flaJ* of the archaeon *Methanococcus voltae* are deficient in flagellum assembly. *Mol Microbiol* 46:879–887
37. VanDyke DJ, Wu J, Ng SY, Kanbe M, Chaban B, Aizawa S, Jarrell KF (2008) Identification of a putative acetyltransferase gene, MMP0350, which affects proper assembly of both flagella and pili in the archaeon *Methanococcus maripaludis*. *J Bacteriol* 190:5300–5307
38. Kelly J, Logan SM, Jarrell KF, VanDyke DJ, Vinogradov E (2009) A novel N-linked flagellar glycan from *Methanococcus maripaludis*. *Carbohydr Res* 344:648–653
39. Ng SY, Wu J, Nair DB, Logan SM, Robotham A, Tessier L, Kelly JF, Uchida K, Aizawa S, Jarrell KF (2011) Genetic and mass spectrometry analyses of the unusual type IV-like pili of the archaeon *Methanococcus maripaludis*. *J Bacteriol* 193:804–814
40. Apolinario EA, Sowers KR (1996) Plate colonization of *Methanococcus maripaludis* and *Methanosarcina thermophila* in a modified canning jar. *FEMS Microbiol Lett* 145:131–137
41. Costa KC, Lie TJ, Jacobs MA, Leigh JA (2013) H<sub>2</sub>-independent growth of the hydrogenotrophic methanogen *Methanococcus maripaludis*. *MBio* 4:e00062-13
42. Lupa B, Hendrickson EL, Leigh JA, Whitman WB (2008) Formate-dependent H<sub>2</sub> production by the mesophilic methanogen *Methanococcus maripaludis*. *Appl Environ Microbiol* 74:6584–6590
43. Whitman WB, Sohn S, Kuk S, Xing R (1987) Role of amino acids and vitamins in nutrition of mesophilic *Methanococcus* spp. *Appl Environ Microbiol* 53:2373–2378
44. Whitman W, Ankwarda E, Wolfe R (1982) Nutrition and carbon metabolism of *Methanococcus voltae*. *J Bacteriol* 149:852–863
45. Lohner ST, Deutzmann JS, Logan BE, Leigh J, Spormann AM (2014) Hydrogenase-independent uptake and metabolism of electrons by the archaeon *Methanococcus maripaludis*. *The ISME journal* 8:1673–1681
46. Lie TJ, Costa KC, Lupa B, Korpole S, Whitman WB, Leigh JA (2012) Essential anaplerotic role for the energy-converting hydrogenase Eha in hydrogenotrophic methanogenesis. *Proc Natl Acad Sci USA* 109:15473–15478
47. Shieh J, Whitman WB (1987) Pathway of acetate assimilation in autotrophic and heterotrophic methanococci. *J Bacteriol* 169:5327–5329
48. Yang Y-L, Ladapo J, Whitman WB (1992) Pyruvate oxidation by *Methanococcus* spp. *Arch Microbiol* 158:271–275
49. White RH (1988) Structural diversity among methanofurans from different methanogenic bacteria. *J Bacteriol* 170:4594–4597
50. Wolfe RS (1985) Unusual coenzymes of methanogenesis. *Trends Biochem Sci* 10:396–399
51. Noll KM, Rinehart KL, Tanner RS, Wolfe RS (1986) Structure of component B (7-mercaptoheptanoylthreonine phosphate) of the methylcoenzyme M methylreductase system of *Methanobacterium thermoautotrophicum*. *Proc Natl Acad Sci* 83:4238–4242
52. Taylor CD, Wolfe RS (1974) Structure and methylation of coenzyme M (HSCH<sub>2</sub>CH<sub>2</sub>SO<sub>3</sub>). *J Biol Chem* 249:4879–4885
53. Hendrickson EL, Leigh JA (2008) Roles of coenzyme F420-reducing hydrogenases and hydrogen- and F420-dependent methylenetetrahydromethanopterin dehydrogenases in reduction of F420 and production of hydrogen during methanogenesis. *J Bacteriol* 190:4818–4821
54. Färber G, Keller W, Kratky C, Jaun B, Pfaltz A, Spinner C, Kobelt A, Eschenmoser A (1991) Coenzyme F430 from methanogenic bacteria: complete assignment of configuration based on an X-Ray analysis of 12, 13-Diepi-F430 pentamethyl ester and on NMR spectroscopy. *Helv Chim Acta* 74:697–716
55. Thauer RK, Kaster AK, Seedorf H, Buckel W, Hedderich R (2008) Methanogenic archaea: ecologically relevant differences in energy conservation. *Nat Rev Microbiol* 6:579–591
56. Thauer RK, Kaster A-K, Goenrich M, Schick M, Hiromoto T, Shima S (2010) Hydrogenases from methanogenic archaea, nickel, a novel cofactor, and H<sub>2</sub> storage. *Annu Rev Biochem* 79:507–536
57. Donnelly M, Wolfe R (1986) The role of formylmethanofuran: tetrahydromethanopterin formyltransferase in methanogenesis from carbon dioxide. *J Biol Chem* 261:16653–16659

58. Mukhopadhyay BSS, Wolfe RS (1998) Purification, regulation, and molecular and biochemical characterization of pyruvate carboxylase from *Methanobacterium thermoautotrophicum* strain  $\Delta$ H. *J Biol Chem* 273:5155–5166
59. Kengen SM DP, Duits EF, Keltjens JT, van der Drift C, Vogels GD (1992) Isolation of a 5-hydroxybenzimidazolyl cobamide-containing enzyme involved in the methyltetrahydromethanopterin: coenzyme M methyltransferase reaction in *Methanobacterium thermoautotrophicum*. *Biochim Biophys Acta* 1118:249–260
60. Kaster A-K, Moll J, Parey K, Thauer RK (2011) Coupling of ferredoxin and heterodisulfide reduction via electron bifurcation in hydrogenotrophic methanogenic archaea. *Proc Natl Acad Sci* 108:2981–2986
61. Major TA, Liu Y, Whitman WB (2010) Characterization of energy-conserving hydrogenase B in *Methanococcus maripaludis*. *J Bacteriol* 192:4022–4030
62. Costa KCLT, Xia Q, Leigh JA (2013) VhuD facilitates electron flow from H<sub>2</sub> or formate to heterodisulfide reductase in *Methanococcus maripaludis*. *J Bacteriol* 195:6160–6165
63. Mitchell P (1974) Chemiosmotic coupling in energy transduction: a logical development of biochemical knowledge. Springer, Berlin
64. Kühn W, Fiebig K, Hippe H, Mah RA, Huser BA, Gottschalk G (1983) Distribution of cytochromes in methanogenic bacteria. *FEMS Microbiol Lett* 20:407–410
65. Muller V, Blaut M, Heise R, Winner C, Gottschalk G (1990) Sodium bioenergetics in methanogens and acetogens. *FEMS Microbiol Lett* 87:373–376
66. Bull AT, Bunch AW, Robinson GK (1999) Biocatalysts for clean industrial products and processes. *Curr Opin Microbiol* 2:246–251
67. Park JH, Lee KH, Kim TY, Lee SY (2007) Metabolic engineering of *Escherichia coli* for the production of L-valine based on transcriptome analysis and in silico gene knockout simulation. *Proc Natl Acad Sci* 104:7797–7802
68. Lewalter K, Müller V (2006) Bioenergetics of archaea: ancient energy conserving mechanisms developed in the early history of life. *Biochim Biophys Acta* 1757:437–445
69. Yang YL, Glushka JN, Whitman WB (2002) Intracellular pyruvate flux in the methane-producing archaeon *Methanococcus maripaludis*. *Arch Microbiol* 178:493–498
70. Lin WC, Yang YL, Whitman WB (2003) The anabolic pyruvate oxidoreductase from *Methanococcus maripaludis*. *Arch Microbiol* 179:444–456
71. Lin W, Whitman WB (2004) The importance of porE and porF in the anabolic pyruvate oxidoreductase of *Methanococcus maripaludis*. *Arch Microbiol* 181:68–73
72. Moore BC, Leigh JA (2005) Markerless mutagenesis in *Methanococcus maripaludis* demonstrates roles for alanine dehydrogenase, alanine racemase, and alanine permease. *J Bacteriol* 187:972–979
73. Lie TJ, Leigh JA (2002) Regulatory response of *Methanococcus maripaludis* to alanine, an intermediate nitrogen source. *J Bacteriol* 184:5301–5306
74. Yu J-P, Ladapo J, Whitman WB (1993) Pathway of glycogen metabolism in *Methanococcus maripaludis*. *J Bacteriol* 176:325–332
75. Sakuraba H, Yoshioka I, Koga S, Takahashi M, Kitahama Y, Satomura T, Kawakami R, Ohshima T (2002) ADP-dependent glucokinase/phosphofructokinase, a novel bifunctional enzyme from the hyperthermophilic archaeon *Methanococcus jannaschii*. *J Biol Chem* 277:12495–12498
76. Castro-Fernandez V, Bravo-Moraga F, Herrera-Morande A, Guixé V (2014) Bifunctional ADP-dependent phosphofructokinase/glucokinase activity in the order Methanococcales—biochemical characterization of the mesophilic enzyme from *Methanococcus maripaludis*. *FEBS J* 281:2017–2029
77. Verhees C, Kengen S, Tuininga J, Schut G, Adams M, de Vos W, Van Der Oost J (2003) The unique features of glycolytic pathways in Archaea. *Biochem J* 375:231–246
78. Siebers B, Schönheit P (2005) Unusual pathways and enzymes of central carbohydrate metabolism in Archaea. *Curr Opin Microbiol* 8:695–705

79. Verhees CH, Huynen MA, Ward DE, Schiltz E, de Vos WM, van der Oost J (2001) The phosphoglucose isomerase from the hyperthermophilic archaeon *Pyrococcus furiosus* is a unique glycolytic enzyme that belongs to the cupin superfamily. *J Biol Chem* 276:40926–40932
80. Graham DE, Xu H, White RH (2002) A divergent archaeal member of the alkaline phosphatase binuclear metalloenzyme superfamily has phosphoglycerate mutase activity. *FEBS Lett* 517:190–194
81. Berg JM, Tymoczko JL, Stryer L (2002) The glycolytic pathway is tightly controlled. In: Freeman WH (ed) *Biochemistry*, 5th edn, Section 16.2, New York. Available from: <http://www.ncbi.nlm.nih.gov/books/NBK22395/>
82. Brunner NA, Siebers B, Hensel R (2001) Role of two different glyceraldehyde-3-phosphate dehydrogenases in controlling the reversible Embden–Meyerhof–Parnas pathway in *Thermoproteus tenax*: regulation on protein and transcript level. *Extremophiles* 5:101–109
83. van der Oost J, Schut G, Kengen SM, Hagen WR, Thomm M, de Vos WM (1998) The ferredoxin-dependent conversion of glyceraldehyde-3-phosphate in the hyperthermophilic archaeon *Pyrococcus furiosus* represents a novel site of glycolytic regulation. *J Biol Chem* 273:28149–28154
84. Ettema TJ, Ahmed H, Geerling AC, van der Oost J, Siebers B (2008) The non-phosphorylating glyceraldehyde-3-phosphate dehydrogenase (GAPN) of *Sulfolobus solfataricus*: a key-enzyme of the semi-phosphorylative branch of the Entner–Doudoroff pathway. *Extremophiles* 12:75–88
85. Park MO, Mizutani T, Jones PR (2007) Glyceraldehyde-3-phosphate ferredoxin oxidoreductase from *Methanococcus maripaludis*. *J Bacteriol* 189:7281–7289
86. Fernie AR, Carrari F, Sweetlove LJ (2004) Respiratory metabolism: glycolysis, the TCA cycle and mitochondrial electron transport. *Curr Opin Plant Biol* 7:254–261
87. Simpson PG, Whitman WB (1993) Anabolic pathways in methanogens. In *Methanogenesis*. Springer, Berlin, pp 445–472
88. Ladapo J, Whitman WB (1990) Method for isolation of auxotrophs in the methanogenic archaeobacteria: role of the acetyl-CoA pathway of autotrophic CO<sub>2</sub> fixation in *Methanococcus maripaludis*. *Proc Natl Acad Sci* 87:5598–5602
89. Lie TJ, Wood GE, Leigh JA (2005) Regulation of nif expression in *Methanococcus maripaludis*: roles of the euryarchaeal repressor NrpR, 2-oxoglutarate, and two operators. *J Biol Chem* 280:5236–5241
90. Dodsworth JA, Cady NC, Leigh JA (2005) 2-Oxoglutarate and the PII homologues NifH1 and NifH2 regulate nitrogenase activity in cell extracts of *Methanococcus maripaludis*. *Mol Microbiol* 56:1527–1538
91. Tumbula DL, Teng Q, Bartlett MG, Whitman WB (1997) Ribose biosynthesis and evidence for an alternative first step in the common aromatic amino acid pathway in *Methanococcus maripaludis*. *J Bacteriol* 179:6010–6013
92. Porat I, Waters BW, Teng Q, Whitman WB (2004) Two biosynthetic pathways for aromatic amino acids in the archaeon *Methanococcus maripaludis*. *J Bacteriol* 186:4940–4950
93. Harmen JG, van de Werken, Brouns SJJ, Oost JVD (2002) Pentose metabolism in archaea. In: Blum P (ed) *Archaea: new models for prokaryotic biology*. Caister Academic Press, Norfolk, pp 71–95
94. Berg JM, Tymoczko JL, Stryer L (2006) *Biochemistry: international edition*. WH Freeman & Company Limited, London
95. Kessler PS, McLarnan J, Leigh JA (1997) Nitrogenase phylogeny and the molybdenum dependence of nitrogen fixation in *Methanococcus maripaludis*. *J Bacteriol* 179:541–543
96. Cohen-Kupiec R, CA Marx, Leigh J (1999) Function and regulation of glnA in the methanogenic archaeon *Methanococcus maripaludis*. *J Bacteriol* 18:256–261
97. Pine MJ, Barker H (1954) Studies of the methane bacteria: XI. Fixation of atmospheric nitrogen by *Methanobacterium omelianskii*. *J Bacteriol* 68:589

98. Belay N, Sparling R, Daniels L (1984) Dinitrogen fixation by a thermophilic methanogenic bacterium, vol 312, pp 286–288
99. Belay N, Sparling R, Choi B-S, Roberts M, Roberts J, Daniels L (1988) Physiological and  $^{15}\text{N}$ -NMR analysis of molecular nitrogen fixation by *Methanococcus thermolithotrophicus*, *Methanobacterium bryantii* and *Methanospirillum hungatei*. *Biochim Biophys Acta* 971:233–245
100. Kendall MM, Liu Y, Sieprawska-Lupa M, Stetter KO, Whitman WB, Boone DR (2006) *Methanococcus aeolicus* sp. nov., a mesophilic, methanogenic archaeon from shallow and deep marine sediments. *Int J Syst Evol Microbiol* 56:1525–1529
101. Takai K, Nealson KH, Horikoshi K (2004) *Methanotorris formicicus* sp. nov., a novel extremely thermophilic, methane-producing archaeon isolated from a black smoker chimney in the Central Indian Ridge. *Int J Syst Evol Microbiol* 54:1095–1100
102. Blank CE, Kessler PS, Leigh JA (1995) Genetics in methanogens: transposon insertion mutagenesis of a *Methanococcus maripaludis* nifH gene. *J Bacteriol* 177:5773–5777
103. Kessler PS, Blank C, Leigh JA (1998) The nif gene operon of the methanogenic archaeon *Methanococcus maripaludis*. *J Bacteriol* 180:1504–1511
104. Huber H, Thomm M, König H, Thies G, Stetter KO (1982) *Methanococcus thermolithotrophicus*, a novel thermophilic lithotrophic methanogen. *Arch Microbiol* 132:47–50
105. Dodge E (2014) Carbon dioxide can be a resource rather than a waste product. <http://www.theenergycollective.com/ed-dodge/341971>
106. Kessler PS, Daniel C, Leigh JA (2001) Ammonia switch-off of nitrogen fixation in the methanogenic archaeon *Methanococcus maripaludis*: mechanistic features and requirement for the novel GlnB homologues, Nif I(1) and NifI(2). *J Bacteriol* 183:882–889
107. Lie TJ, Leigh JA (2002) A novel repressor of nif and glnA expression in the methanogenic archaeon *Methanococcus maripaludis*. *Mol Microbiol* 47:235–246
108. Kessler PS, Leigh JA (1999) Genetics of nitrogen regulation in *Methanococcus maripaludis*. *Genetics* 152:1343–1351
109. Xing R, Whitman WB (1991) Characterization of enzymes of the branched-chain amino acid biosynthetic pathway in *Methanococcus* spp. *J Bacteriol* 173:2086–2092
110. Smith DR, Doucette-Stamm LA, Deloughery C, Lee H, Dubois J, Aldredge T, Bashirzadeh R, Blakely D, Cook R, Gilbert K (1997) Complete genome sequence of *Methanobacterium thermoautotrophicum* deltaH: functional analysis and comparative genomics. *J Bacteriol* 179:7135
111. Graupner M, White RH (2001) *Methanococcus jannaschii* generates l-proline by cyclization of L-ornithine. *J Bacteriol* 183:5203–5205
112. Porat I, Sieprawska-Lupa M, Teng Q, Bohanon FJ, White RH, Whitman WB (2006) Biochemical and genetic characterization of an early step in a novel pathway for the biosynthesis of aromatic amino acids and p-aminobenzoic acid in the archaeon *Methanococcus maripaludis*. *Mol Microbiol* 62:1117–1131
113. Fondi M, Emiliani G, Lio P, Gribaldo S, Fani R (2009) The evolution of histidine biosynthesis in archaea: insights into the his genes structure and organization in LUCA. *J Mol Evol* 69:512–526
114. Liu Y (2010) Adaptations of *Methanococcus maripaludis* to its unique lifestyle. The University of Georgia, Georgia
115. Meile L, Leisinger T (1984) Enzymes of arginine biosynthesis in methanogenic bacteria. *Experientia* 40:899–900
116. Cohen-Kupiec R, Kupiec M, Sandbeck K, Leigh J (1999) Functional conservation between the argininosuccinate lyase of the archaeon *Methanococcus maripaludis* and the corresponding bacterial and eukaryal genes. *FEMS Microbiol Lett* 173:231–238
117. Kenealy WR, Zeikus J (1982) One-carbon metabolism in methanogens: evidence for synthesis of a two-carbon cellular intermediate and unification of catabolism and anabolism in *Methanosarcina barkeri*. *J Bacteriol* 151:932–941



118. Stathopoulos C, Kim W, Li T, Anderson I, Deutsch B, Palioura S, Whitman W, Soll D (2001) Cysteineyl-tRNA synthetase is not essential for viability of the archaeon *Methanococcus maripaludis*. *Proc Natl Acad Sci USA* 98:14292–14297
119. Sauerwald A, Zhu W, Major TA, Roy H, Palioura S, Jahn D, Whitman WB, Yates JR 3rd, Ibba M, Söll D (2005) RNA-dependent cysteine biosynthesis in archaea. *Science* 307:1969–1972
120. Zhang C-M, Liu C, Slater S, Hou Y-M (2008) Aminoacylation of tRNA with phosphoserine for synthesis of cysteinyl-tRNA<sup>Cys</sup>. *Nat Struct Mol Biol* 15:507–514
121. Turanov AA, Xu X-M, Carlson BA, Yoo M-H, Gladyshev VN, Hatfield DL (2011) Biosynthesis of selenocysteine, the 21st amino acid in the genetic code, and a novel pathway for cysteine biosynthesis. *Adv Nutr Intl Rev J* 2:122–128
122. Yuan J, Palioura S, Salazar JC, Su D, O'Donoghue P, Hohn MJ, Cardoso AM, Whitman WB, Söll D (2006) RNA-dependent conversion of phosphoserine forms selenocysteine in eukaryotes and archaea. *Proc Natl Acad Sci* 103:18923–18927
123. Hohn MJ, Palioura S, Su D, Yuan J, Söll D (2011) Genetic analysis of selenocysteine biosynthesis in the archaeon *Methanococcus maripaludis*. *Mol Microbiol* 81:249–258
124. Stock T, Selzer M, Connery S, Seyhan D, Resch A, Rother M (2011) Disruption and complementation of the selenocysteine biosynthesis pathway reveals a hierarchy of selenoprotein gene expression in the archaeon *Methanococcus maripaludis*. *Mol Microbiol* 82:734–747
125. Rother M, Mathes I, Lottspeich F, Böck A (2003) Inactivation of the selB gene in *Methanococcus maripaludis*: effect on synthesis of selenoproteins and their sulfur-containing homologs. *J Bacteriol* 185:107–114
126. Srinivasan G, James CM, Krzycki JA (2002) Pyrrolysine encoded by UAG in archaea: charging of a UAG-decoding specialized tRNA. *Science* 296:1459–1462
127. Alkalaeva E, Eliseev B, Ambrogelly A, Vlasov P, Kondrashov FA, Gundllapalli S, Frolova L, Söll D, Kisselev L (2009) Translation termination in pyrrolysine-utilizing archaea. *FEBS Lett* 583:3455–3460
128. Leigh JA, Albers SV, Atomi H, Allers T (2011) Model organisms for genetics in the domain archaea: methanogens, halophiles, thermococcales and sulfolobales. *FEMS Microbiol Rev* 35:577–608
129. Sarmiento FB, Leigh JA, Whitman WB (2011) Genetic systems for hydrogenotrophic methanogens. *Methods Enzymol* 494:43–73
130. Argyle JL, Tumbula DL, Leigh JA (1996) Neomycin resistance as a selectable marker in *Methanococcus maripaludis*. *Appl Environ Microbiol* 62:4233–4237
131. Sandbeck KA, Leigh JA (1991) Recovery of an integration shuttle vector from tandem repeats in *Methanococcus maripaludis*. *Appl Environ Microbiol* 57:2762–2763
132. Lie TJ, Leigh JA (2007) Genetic screen for regulatory mutations in *Methanococcus maripaludis* and its use in identification of induction-deficient mutants of the euryarchaeal repressor NrpR. *Appl Environ Microbiol* 73:6595–6600
133. Tumbula DL, Makula RA, Whitman WB (1994) Transformation of *Methanococcus maripaludis* and identification of a Pst I-like restriction system. *FEMS Microbiol Lett* 121:309–314
134. GIBCO B: Product catalogue and reference guide. Life Technologies Inc.
135. Weisburg WG, Tanner RS (1982) Aminoglycoside sensitivity of archaeobacteria. *FEMS Microbiol Lett* 14:307–310
136. Tumbula DL, Bowen TL, Whitman WB (1997) Characterization of pURB500 from the archaeon *Methanococcus maripaludis* and construction of a shuttle vector. *J Bacteriol* 179:2976–2986
137. Gardner WL, Whitman W (1999) Expression vectors for *Methanococcus maripaludis* overexpression of acetohydroxyacid synthase and  $\beta$ -galactosidase. *Genet Soc Am* 152:1439–1447

138. Walters AD, Smith SE, Chong JP (2011) Shuttle vector system for *Methanococcus maripaludis* with improved transformation efficiency. *Appl Environ Microbiol* 77: 2549–2551
139. Kim W, Whitman WB (1999) Isolation of acetate auxotrophs of the methane-producing archaeon *Methanococcus maripaludis* by random insertional mutagenesis. *Genetics* 152:1429–1437
140. Tabatabaei M, Rahim RA, Abdullah N, Wright A-DG, Shirai Y, Sakai K, Sulaiman A, Hassan MA (2010) Importance of the methanogenic archaea populations in anaerobic wastewater treatments. *Process Biochem* 45:1214–1225
141. Ali Shah F, Mahmood Q, Maroof Shah M, Pervez A, Ahmad Asad S (2014) Microbial ecology of anaerobic digesters: the key players of anaerobiosis. *Sci World J* 183752:21. doi:[10.1155/2014/183752](https://doi.org/10.1155/2014/183752)
142. Song C (2003) An overview of new approaches to deep desulfurization for ultra-clean gasoline, diesel fuel and jet fuel. *Catal Today* 86:211–263
143. Arsova L (2010) Anaerobic digestion of food waste: Current status, problems and an alternative product. Columbia University, New York
144. Morita M, Malvankar NS, Franks AE, Summers ZM, Giloteaux L, Rotaru AE, Rotaru C, Lovley DR (2011) Potential for direct interspecies electron transfer in methanogenic wastewater digester aggregates. *MBio* 2:e00159–00111
145. Summers ZM, Fogarty HE, Leang C, Franks AE, Malvankar NS, Lovley DR (2010) Direct exchange of electrons within aggregates of an evolved syntrophic coculture of anaerobic bacteria. *Science* 330:1413–1415
146. Rotaru AE, Mallaá Shrestha P, Liu F, Shrestha M, Shrestha D, Embree M, Zengler K, Wardman C, Nevin KP, Lovley DR (2014) A new model for electron flow during anaerobic digestion: direct interspecies electron transfer to Methanosaeta for the reduction of carbon dioxide to methane. *Energy Environ Sci* 7:408–415
147. Aaron D, Tsouris C (2005) Separation of CO<sub>2</sub> from flue gas: a review. *Sep Sci Technol* 40:321–348
148. Marshall CW, Ross DE, Fichot EB, Norman RS, May HD (2012) Electrosynthesis of commodity chemicals by an autotrophic microbial community. *Appl Environ Microbiol* 78:8412–8420
149. Wu K, Birgersson E, Kim B, Kenis PJ, Karimi IA (2015) Modeling and experimental validation of electrochemical reduction of CO<sub>2</sub> to CO in a microfluidic cell. *J Electrochem Soc* 162:F23–F32
150. Nandi R, Sengupta S (1998) Microbial production of hydrogen: an overview. *Crit Rev Microbiol* 24:61–84
151. Kuhn M, Steinbüchel A, Schlegel HG (1984) Hydrogen evolution by strictly aerobic hydrogen bacteria under anaerobic conditions. *J Bacteriol* 159:633–639
152. Yoshida A, Nishimura T, Kawaguchi H, Inui M, Yukawa H (2005) Enhanced hydrogen production from formic acid by formate hydrogen lyase-overexpressing *Escherichia coli* strains. *Appl Environ Microbiol* 71:6762–6768
153. Valentine DL, Blanton DC, Reeburgh WS (2000) Hydrogen production by methanogens under low-hydrogen conditions. *Arch Microbiol* 174:415–421
154. Modification of *Methanococcus maripaludis* for production of geraniol. <http://2012.igem.org/files/presentation/UGA-Georgia.pdf>
155. Boopathy R (1996) Methanogenic transformation of methylfurfural compounds to furfural. *Appl Environ Microbiol* 62:3483–3485
156. Boopathy R, Kulpa CF (1994) Biotransformation of 2, 4, 6-trinitrotoluene (TNT) by a *Methanococcus* sp. (strain B) isolated from a lake sediment. *Can J Microbiol* 40:273–278
157. Moore BC, Leigh JA (2005) Markerless mutagenesis in *Methanococcus maripaludis* demonstrates roles for alanine dehydrogenase, alanine racemase, and alanine permease. *J Bacteriol* 187:972–979
158. Cohen SN, Chang AC, Boyer HW, Helling RB (1973) Construction of biologically functional bacterial plasmids in vitro. *Proc Natl Acad Sci* 70:3240–3244

159. Ribaut J, de Vicente M, Delannay X (2010) Molecular breeding in developing countries: challenges and perspectives. *Curr Opin Plant Biol* 13:213–218
160. Liao JC, Hou SY, Chao YP (1996) Pathway analysis, engineering, and physiological considerations for redirecting central metabolism. *Biotechnol Bioeng* 52:129–140
161. Stephanopoulos G (1999) Metabolic fluxes and metabolic engineering. *Metab Eng* 1:1–11
162. Park JH, Lee SY (2008) Towards systems metabolic engineering of microorganisms for amino acid production. *Curr Opin Biotechnol* 19:454–460
163. Aldor IS, Keasling JD (2003) Process design for microbial plastic factories: metabolic engineering of polyhydroxyalkanoates. *Curr Opin Biotechnol* 14:475–483
164. Shintani D, DellaPenna D (1998) Elevating the vitamin E content of plants through metabolic engineering. *Science* 282:2098–2100
165. Singh SP, Zhou X-R, Liu Q, Stymne S, Green AG (2005) Metabolic engineering of new fatty acids in plants. *Curr Opin Plant Biol* 8:197–203
166. Khosla C, Keasling JD (2003) Metabolic engineering for drug discovery and development. *Nat Rev Drug Discovery* 2:1019–1025
167. Thomas S, Mooney P, Burrell M, Fell D (1997) Metabolic control analysis of glycolysis in tuber tissue of potato (*Solanum tuberosum*): explanation for the low control coefficient of phosphofructokinase over respiratory flux. *Biochem J* 322:119–127
168. Krab K (1995) Kinetic and regulatory aspects of the function of the alternative oxidase in plant respiration. *J Bioenerg Biomembr* 27:387–396
169. Pettersson G, Ryde-Pettersson U (1988) A mathematical model of the Calvin photosynthesis cycle. *Eur J Biochem* 175:661–672
170. Luedeking R, Piret EL (1959) A kinetic study of the lactic acid fermentation. Batch process at controlled pH. *J Biochem Microbiol Technol Eng* 1:393–412
171. Lawrence AW, McCarty PL (1969) Kinetics of methane fermentation in anaerobic treatment. *J Water Pollut Control Fed* R1–R17
172. Hynne F, Dano S, Sorensen PG (2001) Full-scale model of glycolysis in *Saccharomyces cerevisiae*. *Biophys Chem* 94:121–163
173. Bakker BM, van Eunen K, Jeneson JA, van Riel NA, Bruggeman FJ, Teusink B (2010) Systems biology from microorganisms to human metabolic diseases-The role of detailed kinetic models. *Biochem Soc Trans* 38:1294
174. Xu X, Pang KS (1989) Hepatic modeling of metabolite kinetics in sequential and parallel pathways: salicylamide and gentisamide metabolism in perfused rat liver. *J Pharmacokin Biopharm* 17:645–671
175. Fleischmann R, Adams M, White O, Clayton R, Tatusov R, Mushegian A, Bork P, Brown N, Hayes W, White O (1995) Whole-genome random sequencing and assembly of *Haemophilus*. *Science* 269:496–512
176. Price ND, Papin JA, Schilling CH, Palsson BO (2003) Genome-scale microbial *in silico* models: the constraints-based approach. *Trends Biotechnol* 21:162–169
177. Terzer M, Maynard ND, Covert MW, Stelling J (2009) Genome-scale metabolic networks. *Syst Biol Med* 3:285–297 (Wiley Interdisciplinary Reviews)
178. Price ND, Reed JL, Palsson BO (2004) Genome-scale models of microbial cells: evaluating the consequences of constraints. *Nat Rev Microbiol* 2:886–897
179. Raman K, Chandra N (2009) Flux balance analysis of biological systems: applications and challenges. *Brief Bioinform* 10:435–449
180. Sherman BT, Huang DW, Tan Q, Guo Y, Bour S, Liu D, Lempicki RA et al (2007) DAVID Knowledgebase: a gene-centered database integrating heterogeneous gene annotation resources to facilitate high-throughput gene functional analysis. *BMC bioinformatics* 8(1):426
181. Schuetz R, Kuepfer L, Sauer U (2007) Systematic evaluation of objective functions for predicting intracellular fluxes in *Escherichia coli*. *Mol Syst Biol* 3:119
182. Burgard AP, Maranas CD (2003) Optimization-based framework for inferring and testing hypothesized metabolic objective functions. *Biotechnol Bioeng* 82:670–677

183. Feist AM, Palsson BO (2010) The biomass objective function. *Curr Opin Microbiol* 13:344–349
184. Blombach B, Riester T, Wieschalka S, Ziert C, Youn J-W, Wendisch VF, Eikmanns BJ (2011) *Corynebacterium glutamicum* tailored for efficient isobutanol production. *Appl Environ Microbiol* 77:3300–3310
185. Lakshmanan M, Koh G, Chung BK, Lee D-Y (2014) Software applications for flux balance analysis. *Briefings Bioinform* 15:108–122
186. Lee J, Yun H, Feist AM, Palsson BO, Lee SY (2008) Genome-scale reconstruction and in silico analysis of the *Clostridium acetobutylicum* ATCC 824 metabolic network. *Appl Microbiol Biotechnol* 80:849–862
187. Vallino JJ, Stephanopoulos G (1994) Carbon flux distributions at the pyruvate branch point in *Corynebacterium glutamicum* during lysine overproduction. *Biotechnol Prog* 10:320–326
188. Collins D, Briggs D, Morris SC (1983) Expression of naphthalene oxidation genes in *Escherichia coli* results in the biosynthesis of indigo. *Science* 222:167–69
189. Tong I-T, Liao HH, Cameron D (1991) 1, 3-Propanediol production by *Escherichia coli* expressing genes from the *Klebsiella pneumoniae* dha regulon. *Appl Environ Microbiol* 57:3541–3546
190. Aggarwal S, Karimi IA, Lee DY (2011) Reconstruction of a genome-scale metabolic network of *Rhodococcus erythropolis* for desulfurization studies. *Mol BioSyst* 7:3122–3131
191. Tsunekawa H, Azuma S, Okabe M, Okamoto R, Aiba S (1992) Acquisition of a sucrose utilization system in *Escherichia coli* K-12 derivatives and its application to industry. *Appl Environ Microbiol* 58:2081–2088
192. Hollenberg CP, Strasser AWM (1990) Improvement of baker's and brewer's yeast by gene technology. *J Food Biotechnol* 4(1):527–534
193. Lee J-Y, Jung K-H, Choi SH, Kim H-S (1995) Combination of the tod and the tol pathways in redesigning a metabolic route of *Pseudomonas putida* for the mineralization of a benzene, toluene, and p-xylene mixture. *Appl Environ Microbiol* 61:2211–2217
194. Islam MA, Edwards EA, Mahadevan R (2010) Characterizing the metabolism of *Dehalococcoides* with a constraint-based model. *PLoS Comput Biol* 6:e1000887
195. Kallio PT, Kim D, Tsai PS, Bailey JE (1994) Intracellular expression of *Vitreoscilla* hemoglobin alters *Escherichia coli* energy metabolism under oxygen-limited conditions. *Eur J Biochem* 219:201–208
196. Goyal N, Widiastuti H, Karimi IA, Zhou Zhi G (2013) Genome-scale metabolic network reconstruction and in silico analysis of *Methanococcus maripaludis* S2. In: Andrzej K, Ilkka T (eds) *Computer aided chemical engineering*. Elsevier, Amsterdam, vol 32, pp 181–186
197. Windass J, Worsey M, Pioli E, Pioli D, Barth P, Atherton K, Dart E, Byrom D, Powell K, Senior P (1980) Improved conversion of methanol to single-cell protein by *Methylophilus methylotrophus*. *Nature* 287:396–401
198. Resendis-Antonio O, Reed JL, Encarnación S, Collado-Vides J, Palsson BØ (2007) Metabolic reconstruction and modeling of nitrogen fixation in *Rhizobium etli*. *PLoS Comput Biol* 3:e192
199. Stolyar S, Van Dien S, Hillesland KL, Pinel N, Lie TJ, Leigh JA, Stahl DA (2007) Metabolic modeling of a mutualistic microbial community. *Mol Syst Biol* 3:92
200. Henry CS, DeJongh M, Best AA, Frybarger PM, Linsay B, Stevens RL (2010) High-throughput generation, optimization and analysis of genome-scale metabolic models. *Nat Biotechnol* 28:977–982
201. Goyal N, Widiastuti H, Karimi IA, Zhou Z (2014) Genome-scale metabolic model of *Methanococcus maripaludis* S2 for CO<sub>2</sub> capture and conversion to methane. *Mol BioSyst* 10:1043–1054
202. Sarmiento F, Mrázek J, Whitman WB (2013) Genome-scale analysis of gene function in the hydrogenotrophic methanogenic archaeon *Methanococcus maripaludis*. *Proc Natl Acad Sci* 110:4726–4731

203. Rabaey K, Rodriguez J, Blackall LL, Keller J, Gross P, Batstone D, Verstraete W, Nealsen KH (2007) Microbial ecology meets electrochemistry: electricity-driven and driving communities. *ISME J* 1:9–18
204. Logan BE, Hamelers B, Rozendal R, Schröder U, Keller J, Freguia S, Aelterman P, Verstraete W, Rabaey K (2006) Microbial fuel cells: methodology and technology. *Environ Sci Technol* 40:5181–5192
205. Nie H, Zhang T, Cui M, Lu H, Lovley DR, Russell TP (2013) Improved cathode for high efficient microbial-catalyzed reduction in microbial electrosynthesis cells. *Phys Chem Chem Phys* 15:14290–14294
206. Nevin KP, Woodard TL, Franks AE, Summers ZM, Lovley DR (2010) Microbial electrosynthesis: feeding microbes electricity to convert carbon dioxide and water to multicarbon extracellular organic compounds. *MBio* 1:e00103-10.
207. Park D, Laivenieks M, Guettler M, Jain M, Zeikus J (1999) Microbial utilization of electrically reduced neutral red as the sole electron donor for growth and metabolite production. *Appl Environ Microbiol* 65:2912–2917
208. Hongo M, Iwahara M (1979) Application of electro-energizing method to L-glutamic acid fermentation. *Agr Biol Chem* 43:2075–2081
209. Cheng S, Xing D, Call DF, Logan BE (2009) Direct biological conversion of electrical current into methane by electromethanogenesis. *Environ Sci Technol* 43:3953–3958
210. Nevin KP, Hensley SA, Franks AE, Summers ZM, Ou J, Woodard TL, Snoeyenbos-West OL, Lovley DR (2011) Electrosynthesis of organic compounds from carbon dioxide is catalyzed by a diversity of acetogenic microorganisms. *Appl Environ Microbiol* 77:2882–2886
211. Rabaey K, Rozendal RA (2010) Microbial electrosynthesis—revisiting the electrical route for microbial production. *Nat Rev Microbiol* 8:706–716
212. Soleimani M, Bassi A, Margaritis A (2007) Biodesulfurization of refractory organic sulfur compounds in fossil fuels. *Biotechnol Adv* 25:570–596
213. Rozendal RA, Hamelers HV, Molenkamp RJ, Buisman CJ (2007) Performance of single chamber biocatalyzed electrolysis with different types of ion exchange membranes. *Water Res* 41:1984–1994
214. Clauwaert P, Verstraete W (2009) Methanogenesis in membraneless microbial electrolysis cells. *Appl Microbiol Biotechnol* 82:829–836
215. Porat I, Kim W, Hendrickson EL, Xia Q, Zhang Y, Wang T, Taub F, Moore BC, Anderson IJ, Hackett M et al (2006) Disruption of the operon encoding Ehb hydrogenase limits anabolic CO<sub>2</sub> assimilation in the archaeon *Methanococcus maripaludis*. *J Bacteriol* 188:1373–1380

In silico Modeling and Experimental Validation for  
Improving Methanogenesis from CO<sub>2</sub> via *M. maripaludis*  
Goyal, N.

2016, XXV, 122 p. 32 illus., 5 illus. in color., Hardcover  
ISBN: 978-981-10-2509-9